

An Integrated in Silico 3D Model-Driven Discovery of a Novel, Potent, and Selective Amidosulfonamide 5-HT_{1A} Agonist (PRX-00023) for the Treatment of Anxiety and Depression

Oren M. Becker,^{†,*} Dale S. Dhanoa,^{‡,*} Yael Marantz,[†] Dongli Chen,[‡] Sharon Shacham,[†] Srinivasa Cheruku,[‡] Alexander Heifetz,[†] Pradyumna Mohanty,[‡] Merav Fichman,[†] Anurag Sharadendu,[‡] Raphael Nudelman,[†] Michael Kauffman,[‡] and Silvia Noiman[†]

Predix Pharmaceuticals Ltd., 3 Hayetzira Street, Ramat Gan 52521, Israel, and Predix Pharmaceuticals Inc., 4 Maguire Road, Lexington, Massachusetts 02421

Received August 31, 2005

We report the discovery of a novel, potent, and selective amidosulfonamide nonazapirone 5-HT_{1A} agonist for the treatment of anxiety and depression, which is now in Phase III clinical trials for generalized anxiety disorder (GAD). The discovery of **20m** (PRX-00023), *N*-{3-[4-(4-cyclohexylmethanesulfonylaminobutyl)-piperazin-1-yl]phenyl}acetamide, and its backup compounds, followed a new paradigm, driving the entire discovery process with in silico methods and seamlessly integrating computational chemistry with medicinal chemistry, which led to a very rapid discovery timeline. The program reached clinical trials within less than 2 years from initiation, spending less than 6 months in lead optimization with only 31 compounds synthesized. In this paper we detail the entire discovery process, which started with modeling the 3D structure of 5-HT_{1A} using the PREDICT methodology, and then performing in silico screening on that structure leading to the discovery of a 1 nM lead compound (**8**). The lead compound was optimized following a strategy devised based on in silico 3D models and realized through an in silico-driven optimization process, rapidly overcoming selectivity issues (affinity to 5-HT_{1A} vs α 1-adrenergic receptor) and potential cardiovascular issues (hERG binding), leading to a clinical compound. Finally we report key in vivo preclinical and Phase I clinical data for **20m** tolerability, pharmacokinetics, and pharmacodynamics and show that these favorable results are a direct outcome of the properties that were ascribed to the compound during the rational structure-based discovery process. We believe that this is one of the first examples for a Phase III drug candidate that was discovered and optimized, from start to finish, using in silico model-based methods as the primary tool.

Introduction

Serotonin (5-hydroxytryptamine or 5-HT) is involved in a variety of physiological functions such as vasoconstriction,¹ thermoregulation, sexual behavior, pain, appetite, and sleep.^{2–4} In addition, 5-HT-based mechanisms are implicated in neuropsychiatric disturbances such as depression, anxiety, and psychosis.^{5,6} The numerous and varied actions of 5-HT are mediated through 14 receptor subtypes.^{7,8} One of the most actively studied 5-HT receptor subtypes, 5-HT_{1A}, is a 46 kDa, 421 amino acid protein coded on human chromosome 5 by an intronless gene. 5-HT_{1A} receptors are expressed in the CNS with highest density in the dorsal and median raphe nuclei as well as in the hippocampus. High density is also seen in the frontal cortex, entorhinal cortex, amygdale, and septum.

5-HT_{1A} agonists and partial agonists have been implicated in and have demonstrated effectiveness in the treatment of anxiety and depression in the clinic.^{9–13} Partial agonists of the 5-HT_{1A} receptor mediate antidepressant activity through an increase in serotonergic neurotransmission. Although the mechanism of action is not yet fully understood, there is substantial evidence that the physiological and behavioral responses are achieved following desensitization of the 5-HT_{1A} receptor-mediated response.¹³

According to the U.S. National Institute of Mental Health, anxiety (in particular generalized anxiety disorder, or GAD) and

depression are the most prevalent mental illnesses. In the US alone an estimated four million adults suffer from GAD and nearly 19 million adults are affected by depressive disorders. Since GAD and depression are often present together, most patients suffering from these disorders are treated with the same drugs.¹⁴ The most commonly used therapies are selective serotonin reuptake inhibitors (SSRIs) and the more recently developed serotonin noradrenaline reuptake inhibitors (SNRIs). These drugs are thought to exert their effects by increasing neurotransmitter availability and transmission. Another class of drugs used for the short-term relief of GAD is benzodiazepines. These sedating agents are controlled substances because of their addictive properties and can be lethal when used in combination with alcohol.

Importantly, most of the drugs used for anxiety and depression suffer from troublesome side effects. SSRIs, which make up 60% of the worldwide antidepressant and antianxiety market, are frequently associated with sexual dysfunction, appetite disturbances, and sleep disorders. Because SSRIs and SNRIs can increase 5-HT levels in the brain, they can indirectly stimulate all serotonergic receptors, some of which are believed to lead to adverse side effects associated with these drugs. The use of benzodiazepines is associated with addiction, dependency, and cognitive impairment.

Another therapeutic alternative for treatment of anxiety and depression is 5-HT_{1A} agonists. Azapirones comprise the major class of 5-HT_{1A} agonists of which buspirone¹⁵ **1** (Buspar) is the only FDA approved 5-HT_{1A} selective agonist currently on the US market for anxiety (Buspar package insert).¹⁶ Buspirone has shown efficacy in randomized controlled trials of GAD for

* To whom correspondence should be addressed: Phone: +972-3-612-8590, Fax: +972-3-612-8528, e-mail: becker@predixpharm.com.

[†] Predix Pharmaceuticals Ltd., Israel.

[‡] Predix Pharmaceuticals Inc., Lexington, MA.

[§] Current address: P.O. Box 265, Del Mar, CA 92014.

Chart 1. Azapirones, 5-HT_{1A} Agonists, Developed for the Treatment of Anxiety and Depression: Buspirone **1**, the Only Marketed Azapirone, Gepirone **2**, Zalospiroone **3**, Ipsapirone **4**, Tandospirone **5**, and Sunepitron **6**

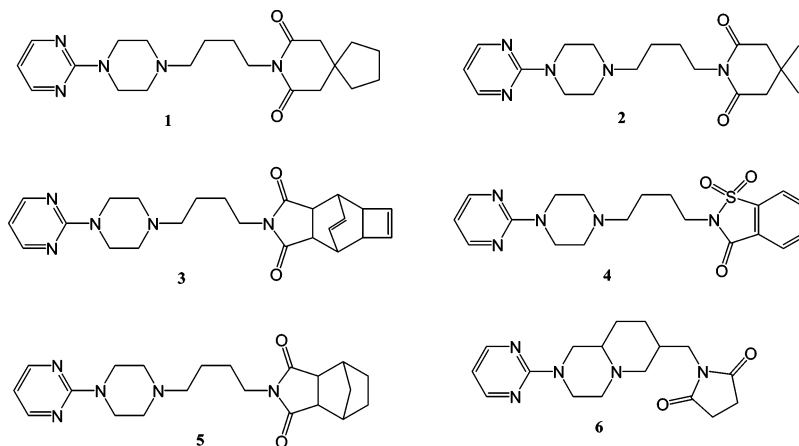


Table 1. Properties of Azapirones and Their Selectivity Profiles

compound	5-HT _{1A} K _i [nM]	α ₁ K _i [nM]	5-HT _{1A} /α ₁ ratio	D2 K _i [nM]	5-HT _{1A} /D2 ratio	dizziness, nausea, headache	human half-life (dosing)
buspirone	20	367	18	13	0.7	yes	2 h (3× daily)
ipsapirone	6	229	38	110	18	yes	2 h (3× daily)
sunepitron	92	35	0.4				2 h (3× daily)
gepiron ER	13	2400	185	58	4	yes	6 h (1× daily)

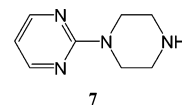
which it was approved.^{17–19} Unlike the benzodiazepines, buspirone is not addictive, even with long-term use. Buspirone also seems to have less pronounced side effects than benzodiazepines and SSRIs/SNRIs and no withdrawal effects, even when the drug is discontinued quickly. Sexual dysfunction, very prominent in depressed and anxious patients, and a major side effect of other psychotropic agents, is not associated with 5-HT_{1A} agonist use. Buspirone has been reported to show modest activity in reducing SSRI-induced sexual side effects.^{20,21}

The main disadvantages of buspirone are side effects such as nausea, headache, nervousness, restlessness, dizziness, light headedness, and fatigue. To overcome these side effects, buspirone has to be gradually titrated for several days or weeks until reaching the therapeutic dose, taking weeks for the drug to be fully effective. For these reasons, buspirone is initiated at 5 mg three times daily (tid) or 7.5 mg twice daily (bid) and then escalated gradually to the clinically effective dose of 10 to 20 mg tid. Another limitation of buspirone is its short elimination time in the body (~2 h),^{22,23} necessitating its three-times a day (tid) dosing and making it less appealing compared to the once a day dosing of SSRIs.

The introduction of buspirone prompted attempts by many pharmaceutical companies to develop new azapirone drugs, structurally similar 5-HT_{1A} agonists, with a superior side effect profile and metabolic stability that will allow them to be dosed once daily. Among these new azapirones are drugs such as gepirone **2**, zalospirone **3**, ipsapirone **4**, tandospirone **5**, and sunepitron **6** (Chart 1). Extended release gepirone²⁴ and ipsapirone²⁵ have shown activity in major depressive disorder studies. Tandospirone improved depressed mood, anxiety, and agitation in a pilot study of patients with dementia.²⁶ However, despite their apparent efficacy, most of these drugs have failed to reach the market due to poor tolerability. Only exceptions are tandospirone, which is marketed only in Japan, and gepirone that is still under active development in an extended release (ER) formulation.

Like buspirone, the other azapirones also suffer from rapid metabolism leading to a very short elimination half-life (serum

elimination half-life [$t_{1/2}$] = 2–3 h)^{22,23} and to a three-times daily dosing (Table 1). This short half-life is due to the rapid formation of the pyrimidinepiperazin metabolite **7**, which is a



potent α₂-adrenergic receptor antagonist.²⁷ Even with an extended release formulation the elimination half-life for gepirone ER is only about 6 h.²⁸

Furthermore, it was found that most of these azapirones share a similar side effect profile consisting of dizziness, lightheadedness, fatigue, nausea, nervousness/restlessness, and in some cases also sleep disorders. Close inspection of the pharmacological profiles of different azapirones suggests that the poor tolerability of this class of drugs may be due to lack of selectivity. While the primary target for these drugs is the 5-HT_{1A} receptor, many of them show high affinity also to α₁ adrenergic receptors and to dopamine D2 receptors (Table 1). This lack of selectivity, together with the potent α₂ adrenergic antagonism effect of the azapirones' primary metabolite, **7**, suggests that the side effects of azapirones may be related to α-adrenergic activities (blood pressure) or dopaminergic activities (nausea, restlessness).

Hence, there is still a medical need for new anti-anxiety and antidepressant drugs with improved efficacy for partial/non-responding and noncompliant patients. These new drugs should have a faster onset of action compared to that of SSRIs, SNRIs, and azapirones (two to four weeks), allow once a day dosing, and have a reduced side effects profile. It should not have the same degree of dizziness, lightheadedness, nervousness/restlessness, and fatigue characteristic of azapirones, the sexual dysfunction, sleep disorders, and other side effects associated with SSRIs, nor the addiction, sedation, and dependence which accompany the use of benzodiazepines. The experience gained with buspirone and other azapirones suggest that a nonazapirone 5-HT_{1A} agonist has the potential of fulfilling this desirable

profile provided it is highly selective and metabolically stable. The selectivity should ensure a better side effect profile and should allow reaching the full therapeutic dose on day 1 to enhance onset of action.

Several classes of compounds such as aminotetralins, aryl-alkylamines, ergolines, indolylamines, and arylpiperazines have been reported as 5-HT_{1A} receptor ligands.^{29–36} Most interesting is a series of studies by Lopez-Rodriguez and collaborators^{37–44} who using extensive SAR analysis together with 3D-QSAR models (e.g., CoMFA) have characterized a range of arylpiperazines, mainly focusing on bicyclohydantoin or diketopiperazine analogues. These studies have shown that the pharmacophore part of these molecules is their pyrimidinepiperazine or arylpiperazine part while the rest of the molecule is nonpharmacophoric in nature. The same studies also showed that most of these compounds exhibit high levels of undesirable affinity to α_1 adrenergic receptor, and that it is not trivial to engineer potent compounds that are selective to one or the other, although examples of selective 5-HT_{1A} agonists have been reported. In general, the lack of an X-ray crystallography structure for the 5-HT_{1A} receptor has so far prevented the application of structure-based approaches to the discovery of selective 5-HT_{1A} agonists, although homology-based models, which use the structure of rhodopsin as a template, have been recently used to rationalize some of the data.^{42,44}

To overcome this lack of structural information, which in general has hampered the application of structure based drug discovery to GPCRs, we have developed PREDICT. PREDICT is a unique nonhomology method for modeling the 3D structure of membrane-embedded GPCRs.^{45,46} The resulting 3D structures have been successfully validated for multiple GPCR drug targets and together with *in silico* screening methodologies have repeatedly yielded novel potent lead candidates.^{46,47}

We herein report on the discovery and development of a novel class of potent, selective, and orally bioavailable amidosulfonamides as 5-HT_{1A} agonists for the treatment of anxiety, depression, and possibly also attention deficit hyperactivity disorder (ADHD). The discovery was made by applying a structure-based and *in silico*-driven approach to the discovery and optimization of this class of compounds. The whole discovery process, from *in silico* screening through lead optimization, preclinical, and into clinical studies, was very rapid, requiring the synthesis of only 31 compounds and taking less than 2 years from program initiation to Phase I clinical trial. This compound is now in Phase III clinical trials in GAD after successfully completed phase II clinical trials, showing efficacy and tolerability in patients.

Results and Discussion

Modeling. PREDICT is a GPCR modeling methodology that combines the properties of the protein sequence with those of its membrane environment, without relying on the X-ray structure of rhodopsin as a template. The PREDICT algorithm and methodology were reported in detail elsewhere.^{45,46} Using PREDICT, a 3D model of the 5-HT_{1A} receptor was generated from its amino acid sequence (Swissprot entry 5-HT_{1A}_human). This model was then virtually complexed with serotonin (5-HT) to form a 3D model of the receptor–ligand complex. A binding pocket was easily identified in the extracellular portion of the TM domain, allowing the amine moiety of 5-HT to interact with residue Asp116 in TM3 and its hydroxyl moiety to interact with residue Ser199 in TM5 (Figure 1), both in good agreement with experimental data.^{48–49}

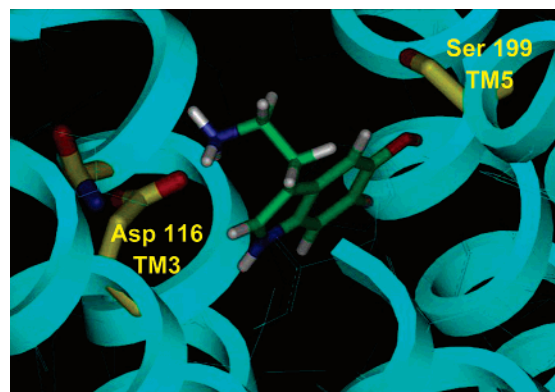


Figure 1. A PREDICT 3D model of the 5-HT_{1A} receptor binding site with a bound 5-HT molecule. Key interactions between the amino group of 5-HT and Asp 116, and between the 5-HT hydroxyl and Ser 199 are highlighted.

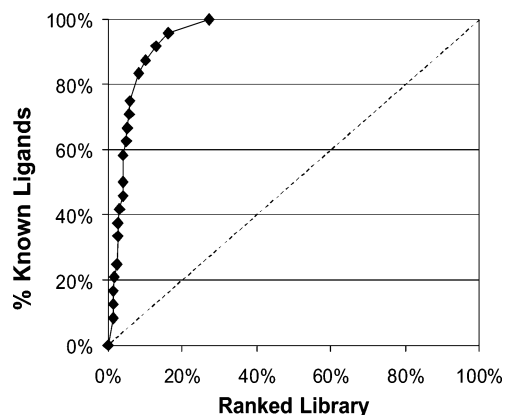


Figure 2. Enrichment graph for *in silico* screening of 34 known 5-HT_{1A} partial agonists embedded in a 10 000-compound random drug-like library with similar physicochemical properties after docking into the PREDICT 3D model of the 5-HT_{1A} receptor. Library compounds are ranked along the *x* axis according to their docking score (best scorers on the left, worst scorers near the 100% mark). Enrichment at 50% is 15-fold better than with random screening (dashed line).

It was previously shown that this 3D model also explains the binding of the azapirones buspirone **1** and sunepitron **6** in the 5-HT_{1A} binding pocket.⁴⁷ In both cases, residue Asp116 is interacting with the piperazine amine and residue Ser199 interacts with the azapirone's imide moiety. In addition, the model shows that residue Phe362 from TM6 stacks against these compounds' pyrimidine rings and that residue Asn386 from TM7 also contributes to this interaction, in agreement with experimental data.⁵⁰

To further validate the model, as well as to calibrate the docking protocol, a virtual 'enrichment' experiment was carried out. Docking a diverse set of 34 known 5-HT_{1A} ligands embedded in a random 10 000 drug-like compound library, with average properties similar to those of the 5-HT_{1A} ligands,⁴⁶ yielded an enrichment factor 15-fold better than random (at the point where 50% of the compounds were identified) when ranked by the initial DOCK score (Figure 2). Furthermore, 90% of the known ligands were ranked among the top 10% of the DOCK-score ranked library.⁴⁵

In Silico Screening. A virtual screening library of 40 000 compounds was extracted from Predix's 2 100 000 compound library. *In silico* docking and scoring of these 40 000 compounds against the 5-HT_{1A} PREDICT model led to the selection of 78 virtual hits. These 78 compounds were purchased from the respective vendors and experimentally tested *in vitro* for binding

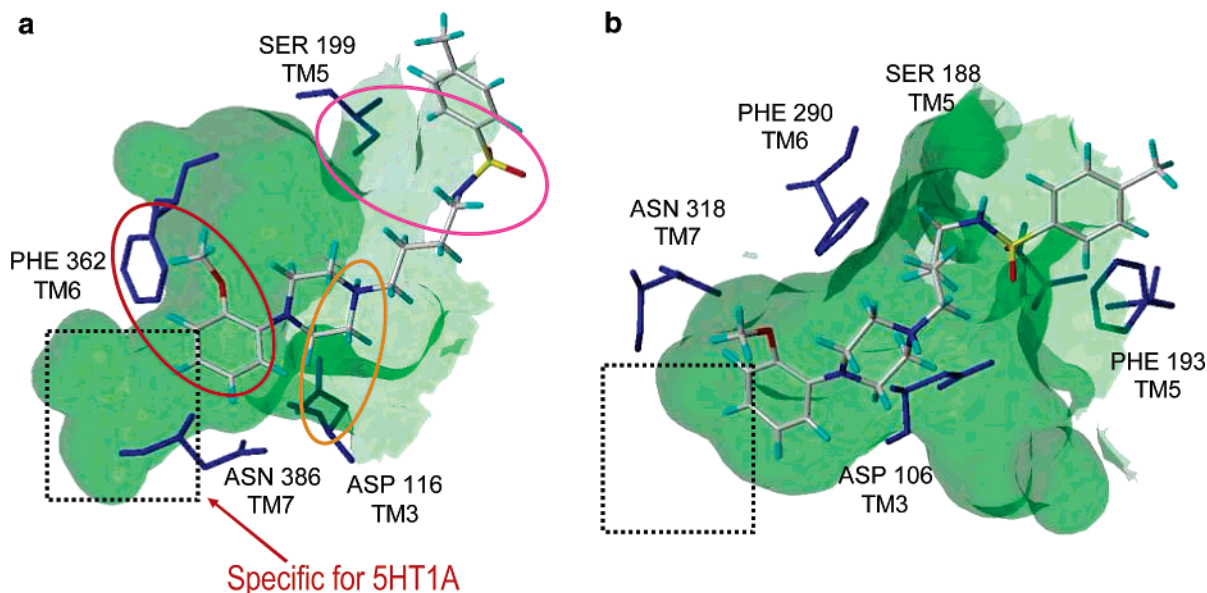
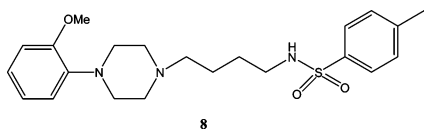


Figure 3. 3D models generated by PREDICT of compound **8** docked into the binding pocket of (a) the 5-HT_{1A} receptor and (b) the α_1 adrenergic receptor. Highlighted are interactions that are formed between the compound and key residues in the binding pocket. The region that is present in the 5-HT_{1A} pocket and is missing in the α_1 pocket is highlighted by a dotted square.

to the 5-HT_{1A} receptor using a radioligand displacement assay. Compounds with experimentally validated binding affinities lower than 5 μ M are defined as actual hits. The in vitro 5-HT_{1A} binding assays confirmed that 16 of the 78 compounds tested were hits with $K_i < 5 \mu$ M, reflecting a 21% hit rate, 9 of which had a $K_i < 1 \mu$ M (K_i values of 1.0, 2.3, 43, 79, 139, 160, 193, 301, and 688 nM, respectively). These 16 compounds represent five distinct chemical scaffolds and 87% of them (14 of 16 compounds) were found to be novel chemical entities, not covered by any patent or publication (other than the supplier's catalog). The best hit was a novel 1.0 nM compound **8**, which was selected as the lead compound for further optimization.



Lead Compound. Arylpiperazinylsulfonamide, **8**, possessed high binding affinity ($K_i = 1.0$ nM) for the 5-HT_{1A} receptor and was tested as a partial agonist in an in vitro cell-based assay (Gi linked to GTP- γ -S), showing 65% activity relative to 5-HT with an EC₅₀ of 21 nM. This functionality compared favorably with buspirone, **1**, the only 5-HT_{1A} partial agonist approved as a drug, which has a 5-HT_{1A} binding K_i of 20 nM, and shows 50% activity relative to 5-HT with an EC₅₀ of \sim 80 nM in a cell-based assay. It also compares well with gepirone, which has a 5-HT_{1A} binding K_i of 13 nM and shows 80% activity relative to 5-HT with an EC₅₀ of \sim 288 nM.

Compound **8** pharmacokinetic (PK) properties in rats are a 1–2 h serum half-life t_{po} and 2% oral bioavailability. Although these PK characteristics are suboptimal for a once a day dosing drug, they are no worse than buspirone **1**, which in rats has a 1 h serum half-life t_{po} and as little as 1% oral bioavailability, and therefore represent a good starting point for lead optimization.

The main downside of compound **8** was its selectivity profile, which like many other 5-HT_{1A} agonists was not selective enough. Testing **8** in vitro against a panel of 50 G-protein coupled receptors showed rather high binding affinities for some of the other receptors, most notably for the adrenergic receptors

α_1 ($K_i = 6$ nM) and α_{2a} ($K_i = 12$ nM), as well as for 5-HT₇ ($K_i = 30$ nM), 5-HT_{2B} ($K_i = 53$ nM), 5-HT transporter ($K_i = 200$ nM), 5-HT_{2A} ($K_i = 490$ nM) and dopamine receptor D₂ ($K_i = 67$ nM). Compound **8** was also tested for cardiovascular safety by assessing its potency for inhibition of the hERG (human ether-a-go-go related gene) K⁺ channel in a patch-clamp assay, yielding an IC₅₀ of > 5000 nM which is considered safe.

Structure-Based in Silico-Driven Optimization. The above battery of in vitro and in vivo assays has shown that the lead compound **8**, which was obtained directly from the in silico screening process, is a novel, potent partial-agonist of 5-HT_{1A}; it is, however, suboptimal in both its pharmacokinetic properties and its selectivity profile. Clearly, both properties had to be optimized. Recalling that the poor tolerability of most azapirones stems from their poor selectivity toward α -adrenergic receptors, we targeted a 5-HT_{1A}/ α_1 selectivity ratio > 200 as the highest priority for this program.

Step 1: Introducing Selectivity for 5-HT_{1A} over α_1 -Adrenergic. The introduction of selectivity toward α -adrenergic receptors while maintaining affinity to 5-HT_{1A} is not an easy task, as has been demonstrated in the extensive research that has been carried out on this topic over the years. Since the α_1 adrenergic receptor is also a GPCR, we used PREDICT to model the 3D structure of the α_1 receptor (Swissprot entry AD1AA_human) complexed with compound **8**, to obtain a structure-based strategy for introducing selectivity. Figure 3 shows compound **8** docked into the two binding pockets of the 5-HT_{1A} and the α_1 adrenergic receptors. According to the 3D model of the 5-HT_{1A} binding pocket (Figure 3a), the aryl moiety of **8** interacts with Phe362 from TM6, the piperazine moiety interacts with Asp116 from TM3, and residue Ser199 interacts with the sulfonamide moiety. This binding mode is very similar to the binding modes of buspirone **1** and of sunepitron **6**, which were discussed above. Interestingly, residue Asn386 from TM7, which contributed to the binding of buspirone, appears not to participate in the binding of **8**.

The 3D model of **8** docked into the binding pocket of the PREDICT generated α_1 adrenergic receptor model (Figure 3b) is also in agreement with its high binding affinity. The aryl

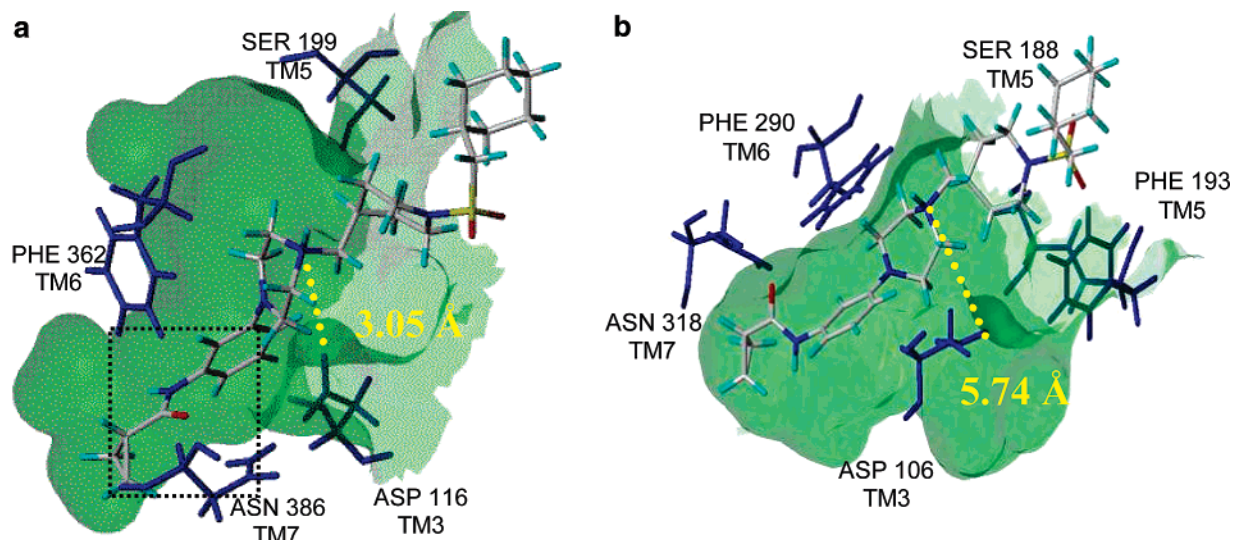
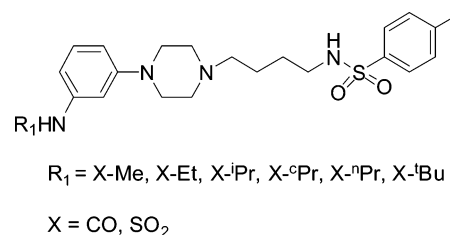


Figure 4. 3D models generated by PREDICT of **20h**, a *m*-^cPrCONH piperidinesulfonyl analogue of **8**, in the binding pockets of (a) 5-HT_{1A} and (b) α₁ receptors. Highlighted are the distances between the piperazine amine atom and the proteins' aspartic acid (Asp116 in 5-HT_{1A} and Asp106 in α₁), indicating that this interaction is maintained in the 5-HT_{1A} structure but lost in the α₁ structure.

moiety of **8** interacts with Phe290 from TM6, the piperazine moiety interacts with Asp106 from TM3, and residues Ser188 and Ser192 interact with the sulfonamide moiety. In addition the 2-OMe group seems to interact with Asn318 from TM7, and the phenyl ring that is attached to the sulfonamide interacts with residue Phe193 from TM5, an interaction that is not observed in the 5-HT_{1A} binding site. This binding mode is in general agreement with putative binding modes suggested in a recently published ligand-supported homology model of α₁, which has yielded very good in silico screening results.⁵¹ Namely, in these 3D models the arylpiperazine (or the pyrimidinedipiperazine) group is embedded deep within the binding pocket in a way that is similar for both 5-HT_{1A} and α₁ receptors, supporting the hypothesis that this part of the molecule contains the pharmacophore.⁴³ Accordingly, the nonpharmacophoric parts of the 5-HT_{1A} ligands, e.g., the imide group of buspirone **1** or the sulfonamide group of **8**, are oriented toward the top of the binding pocket and are less tightly bound.

These two 3D structures were used to outline an optimization strategy for **8** leading to a 5-HT_{1A} over α₁ selectivity. Comparing the two binding sites, one could identify a region near the aryl group that was not occupied by **8** when docked in the 5-HT_{1A} receptor and was missing altogether in the 3D model of α₁. This region is primarily hydrophobic with the exception of residue Asn386, which also contributes to it. According to these 3D structures, replacing the original *o*-OMe group with a bulkier moiety at the meta-position would lead to a more selective compound since this added moiety should bind well to the 5-HT_{1A} pocket but will not fit into the α₁ site. This strategy is in agreement with similar conclusions that were reached using CoMFA analysis³⁸ and Artificial Neural Networks analysis⁴² of a series of bicyclohydantoin-phenylpiperazines with affinity to 5-HT_{1A} and α₁. However, it is of course essential that this group that is expected to reduce the affinity to α₁ will not decrease the activity of the new potential compounds to the target protein, 5-HT_{1A}. Since this additional moiety would bind in a tight region of the 5-HT_{1A} site, its flexibility should be limited in order to minimize the entropic penalty which would reduce its affinity to 5-HT_{1A}. Furthermore, if the new group would have hydrogen donors or acceptors that could interact with Asn386, that added interaction could serve to compensate for the entropic loss as well. The incorporation of *O*-alkyl,

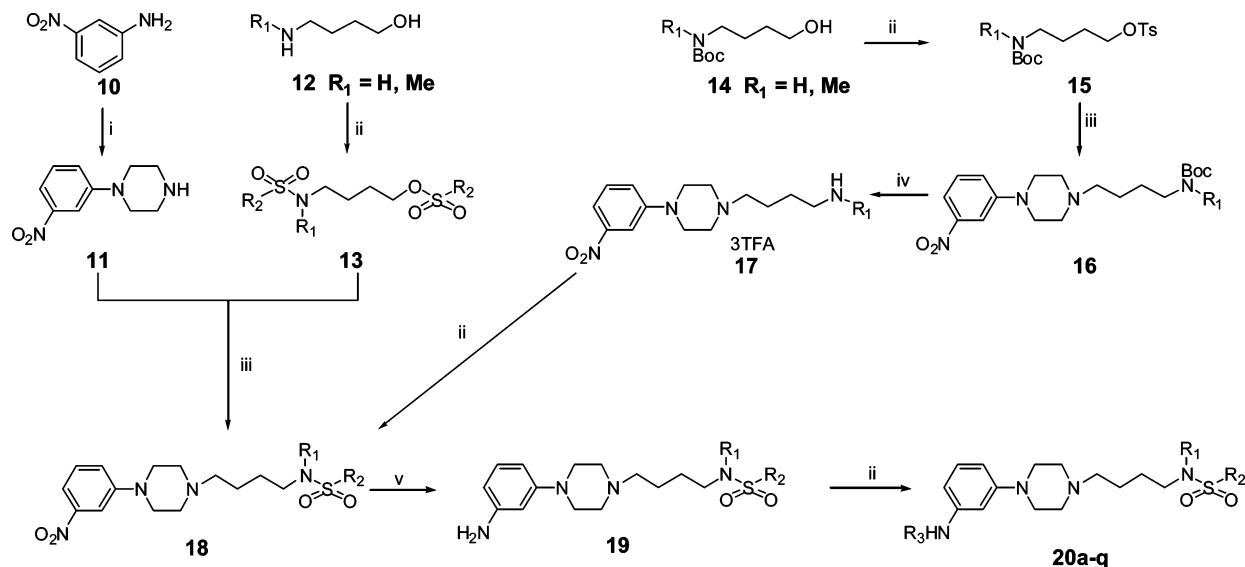
Chart 2. Strategy for Optimization of the Lead Compound **8**



O-aryl, and esters as well as *N*-alkyl substituents was not favored because of the potential propensity of these appendages for metabolic degradation. Hence the strategy that was pursued was to introduce sulfonamides and amides at the meta-position for their metabolic stability. Both groups have been shown in the past to be tolerated at the meta-position of other 5-HT_{1A} ligands.^{41,42} Such amides and sulfonamides groups would potentially have an added value of increasing the compound's solubility and improving its metabolic stability, thus favorably affecting its oral bioavailability and improving the compound's PK profile. A computational analysis of a series of alkyl-amides and alkyl-sulfonamides docked into the 5-HT_{1A} binding site suggested that the maximal size of the alkyl group that can be accommodated at that position was isopropyl or cyclopropyl.

Figure 4 depicts the binding of a *m*-^cPrCONH virtual analogue of **8** in the binding pockets of 5-HT_{1A} and α₁ receptors. As can be seen, this larger moiety at the meta-position does not prevent the compound from docking well into the 5-HT_{1A} binding site, maintaining all the original interactions (e.g., the piperazine-aspartic acid interaction) as well as adding the putative interaction with Asn386 (Figure 4a). On the other hand, according to the 3D model, this bulkier group interferes with binding to α₁, increasing the distance between the piperazine and the aspartic acid to more than 5 Å, effectively preventing this salt-bridge from forming (Figure 4b). Hence the strategy that was selected is depicted in Chart 2. The length of the alkyl linker was not selected for optimization because it has been previously established that maximal affinity for both 5-HT_{1A} and α₁ receptors is reached with a three-carbon or four-carbon linker.^{40–41}

Naturally, even with a well defined strategy, there are multiple compounds that can be proposed for synthesis. To limit the

Scheme 1^a

^a Reagents: (i). $\text{NH}(\text{C}_2\text{H}_4\text{Cl})_2$, Na_2CO_3 , $\text{C}_6\text{H}_5\text{Cl}$, 40–45%; (ii). Et_3N , CH_2Cl_2 , 80–96%; (iii) **11**, Et_3N , THF, 70–76%; (iv) TFA, CH_2Cl_2 , 90%; (v) SnCl_2 , MeOH, HCl, 75%.

number of compounds synthesized, and hence to speed up the optimization process, each proposed compound was computationally analyzed before making a decision whether to synthesize that compound or not. The computational analysis included in silico evaluation of the affinity to 5-HT_{1A}, evaluation of selectivity vs α_1 , and prediction of several ADME properties. In particular, an estimate of the compound's affinity to the target was obtained by docking each proposed compound to the 5-HT_{1A} receptor model and using the resulting binding poses for calculating a predicted 5-HT_{1A} K_i value using a 2D/3D QSAR-based model (in general, $\text{p}K_i$ predictions were accurate to within 0.5 log units). Selectivity was assessed by docking each proposed compounds to the α_1 -adrenergic receptor model and to a 3D model of the hERG channel (see below). ADME-related properties included brain penetration predictions, and other physicochemical parameters such as rotatable bonds, polar surface area, cLogP, and more. The details of these prediction methodologies will be presented elsewhere. These predicted profiles were instrumental in prioritizing and deprioritizing compounds for synthesis, resulting in actual synthesis of only 10% on the proposed compounds.

The selected optimization strategy necessitated the insertion of a pivotal link such as an amino group via which alkyl, aryl, esters, alkylsulfonyl, and acyl groups can be introduced. The synthesis shown in Scheme 1 was developed to allow rapid and efficient preparation as well as scale-up of various compounds shown in Tables 2 and 3. Nitrophenylpiperazine **11** as a common intermediate was prepared by refluxing **10** with bis-(2-chloroethyl)amine chloride salt and Na_2CO_3 in chlorobenzene (Scheme 1). The intermediate **18** was synthesized by two different methods (Scheme 1). In method 1, **18** was directly prepared by treating **11** with **13** which was obtained by disulfonylation of aminobutanol **12**. Compounds **20a–j** and **20p** were synthesized with method 1. In method 2, tosylation products **15** of N-boc-aminobutanol **14** were used as alkylating reagent which reacted with **11** to give boc-protected compounds **16**. Deprotection of compounds **16** by TFA yielded TFA salt **17** which was treated with different sulfonyl chlorides to afford intermediates **18**. Compounds **20k–o** and **20q** were synthesized by method 2. The nitro intermediates **18** were reduced by SnCl_2 in methanol to give corresponding amino compounds **19** with

Table 2. Optimization of Selectivity for 5-HT_{1A} over α -Adrenergic Receptors

compd	R	5-HT _{1A} K_i (nM) ^a	α_1 , %	α_2 , % ^b
8	2-OMe	1.0	6 nM	12 nM
9	H	40	98	90
20a	3-MeSO ₂ NH	46	51	21
20b	3-EtSO ₂ NH	141	47	14
20c	3- ⁱ PrSO ₂ NH	47	47	12
20d	3-MeCONH	6.8	22	43
20e	3-EtCONH	426	0	31
20f	3- ⁿ PrCONH	56	12	12
20g	3- ⁱ PrCONH	78	15	<10
20h	3- ⁿ PrCONH	22	<10	10
20i	3- ^t BuCONH	1360	0	11

^a K_i is the binding affinity determined using h5-HT_{1A} receptor expressed in HEK-293 cells using [³H]8-OH-DPAT as the radioligand (mean value; $n = 2$). ^b % displacement of the radioligand at 1 μM from the α_1 and α_2 adrenergic receptors in rat cerebral cortex cells using [³H]prazosin and [³H]RX 821002, respectively (mean value; $n = 2$).

good yield. The final compounds **20a–q** were obtained by acylation or sulfonylation of intermediates **19** with corresponding acyl chloride and sulfonyl chloride.

Table 2 shows that the resulting structure–activity relationships (SAR) of the sulfonamides **8**, **9**, **20a–i** agree well with the structure-based hypotheses that were laid as the foundation of the optimization strategy. Comparison of the lead compound **8** with the corresponding unsubstituted phenyl analogue **9** showed that presence of the *o*-OMe in **8** affects a 40-fold increase in its 5-HT_{1A} binding affinity with a lesser effect on the activity for both α -adrenergic receptors α_1 and α_2 .

Introducing the alkyl-amides and alkyl-sulfonamides groups at the meta-position significantly reduced the affinity of the compounds to α_1 , moving them from the low nM range (>98% at 1 μM) to the μM range (<50% at 1 μM) for all the compounds **20a–i** in these series. In general the amide series showed greater selectivity toward α_1 with all amide compounds exhibiting α_1 K_i values greater than 3500 nM (<22% at 1 μM), while the sulfonamide compounds exhibited α_1 binding affinities in the vicinity of 1000 nM (~50% at 1 μM).

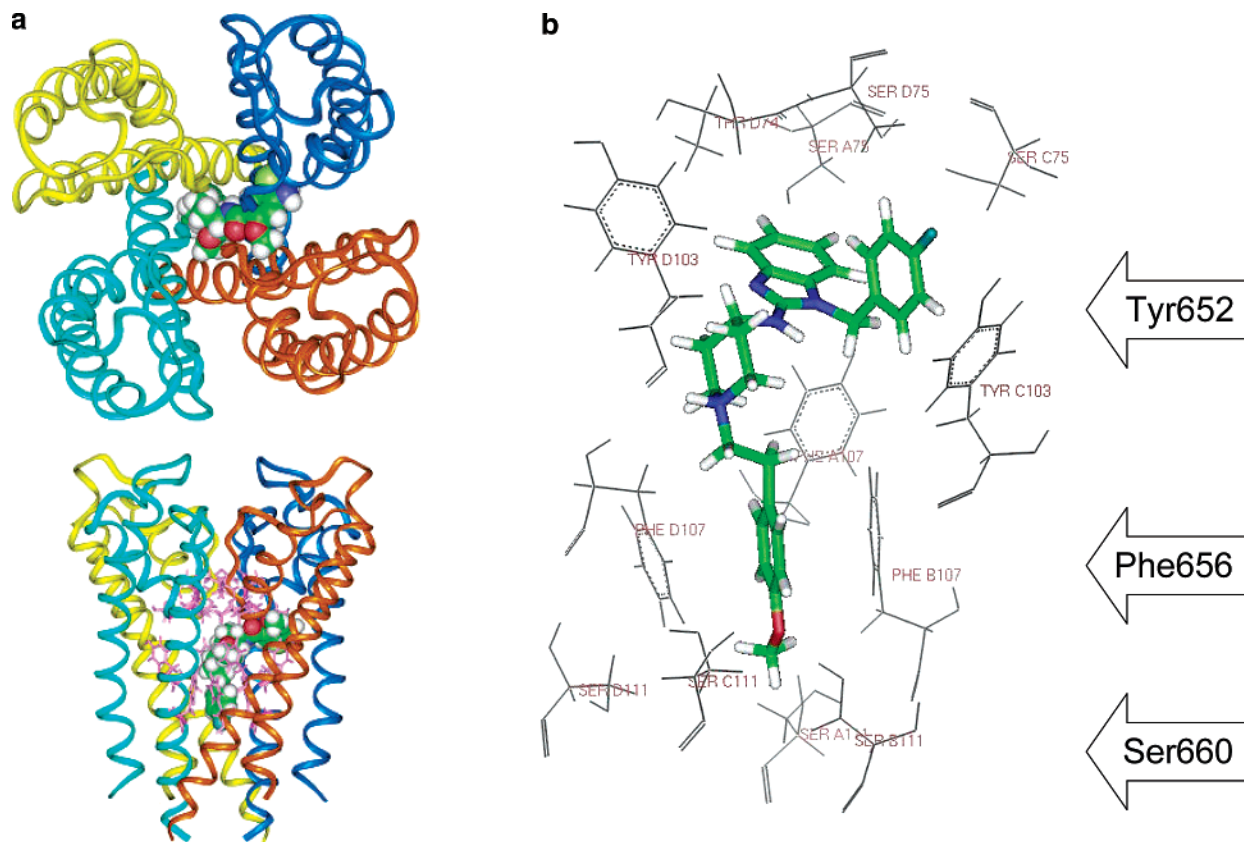


Figure 5. 3D model of the pore forming region (S5–P–S6) of the hERG K⁺ channel with astemizole bound to it (IC₅₀ = 0.9 nM). (a) Top-view and side-view of the hERG tetramer, showing the backbone of each monomer and a space-filling representation of the bound compound. (b) A detailed view of astemizole docked within the hERG channel pore: Phe656 residues are flanking the terminal methoxy-phenyl group of astemizole, Tyr652 residues are within interaction distance from the *p*-fluorophenyl group, and the Ser660 residues are at interaction distance from the terminal methoxy group.

Selectivity toward α_2 was in general commensurate with the selectivity toward α_1 .

The SAR also suggests that alkyl groups ranging in size from Me to Pr were tolerated within the 5-HT_{1A} binding pocket. On the other hand, in agreement with the computational prediction, the bulkier ^tBu group **20i** does not fit in that pocket as reflected by its reduced potency (K_i = 1360 nM). In fact, compound **20i** showed 200-fold less 5-HT_{1A} binding affinity than the most active analogue **20d** (K_i = 6.8 nM).

As expected, the best 5-HT_{1A} K_i values were obtained for analogues which are conformationally the most constrained, MeCONH **20d** (K_i = 6.8 nM), ^cPrCONH **20h** (K_i = 22 nM), and MeSO₂NH **20a** (K_i = 46 nM). Accordingly, higher K_i values were measured for conformationally less constrained analogues, such as EtCONH **20e** (K_i = 426 nM) and EtSO₂NH **20b** (K_i = 141 nM). The effect of entropy can be seen when comparing the propyl series of amide derivatives, **20f**, **20g**, and **20h** substituted with ⁿPr, ⁱPr, and ^cPr, respectively, at the meta-position to the phenyl of piperazine which showed high to moderate binding affinity depending upon the size and volume of the appendage. The ⁿPr and the ⁱPr analogues (K_i = 56 nM and 78 nM, respectively) exhibited 2–3-fold less 5-HT_{1A} binding affinity than the conformationally restricted ^cPr derivative **20h** which demonstrated 5-HT_{1A} K_i of 22 nM and virtually no affinity for adrenergic receptors. It is not clear why the flexible ⁿPr analogue **20f** has a lower K_i than the corresponding ⁱPr compound **20g**; this may be attributed to assay variability or its ability to maximize hydrophobic interactions in that region of the site.

The optimized Me-amide analogue **20d** not only has high 5-HT_{1A} affinity (K_i = 6.8 nM) it also surpassed the target

selectivity goal, exhibiting a 5-HT_{1A}/ α_1 selectivity ratio >500 (α_1 K_i > 3500 nM) and showing partial agonist activity with an EC₅₀ = 20 nM in an in vitro cell-based assay, similar to that of the lead compound **8**. Compound **20d** also demonstrated excellent half-life both in human liver microsomal assay (hLM $t_{1/2}$ = 39 min) and in rat pharmacokinetic evaluation ($t_{1/2}$ = 3.3 h, oral administration), with a rat oral bioavailability of 15%, showing a significant improvement in oral bioavailability compared to the 2% of the lead compound **8**. The observed improvement in oral bioavailability and metabolic stability during the optimization was another validation of the strategy discussed above.

However, when **20d** was examined for its cardiovascular safety there was an unpleasant surprise. While the lead compound **8** exhibited very poor binding to the hERG K⁺ channel (IC₅₀ > 5000 nM), the optimized compound **20d** has become a more potent hERG blocker, inhibiting the channel (when evaluated in a patch-clamp assay) with a IC₅₀ of 300 nM. Since the hERG K⁺ channel is a major regulatory molecular mechanism underlying QT prolongation syndrome,⁵² which is linked to a predisposition of ventricular arrhythmia that can lead to ventricular fibrillation and sudden death,⁵³ hERG blocking is considered a serious hazard which has led to removal from the market of drugs such as azemizole and cisapride.

Step 2: Reducing Affinity to hERG. The high affinity of **20d** to the hERG channel had to be reduced at least 10-fold for a derivative of this compound to reach development candidate status. As in the case of the selectivity profile, we applied a structure-based approach to alleviate the hERG affinity problem. Since there is no experimentally determined X-ray structure of

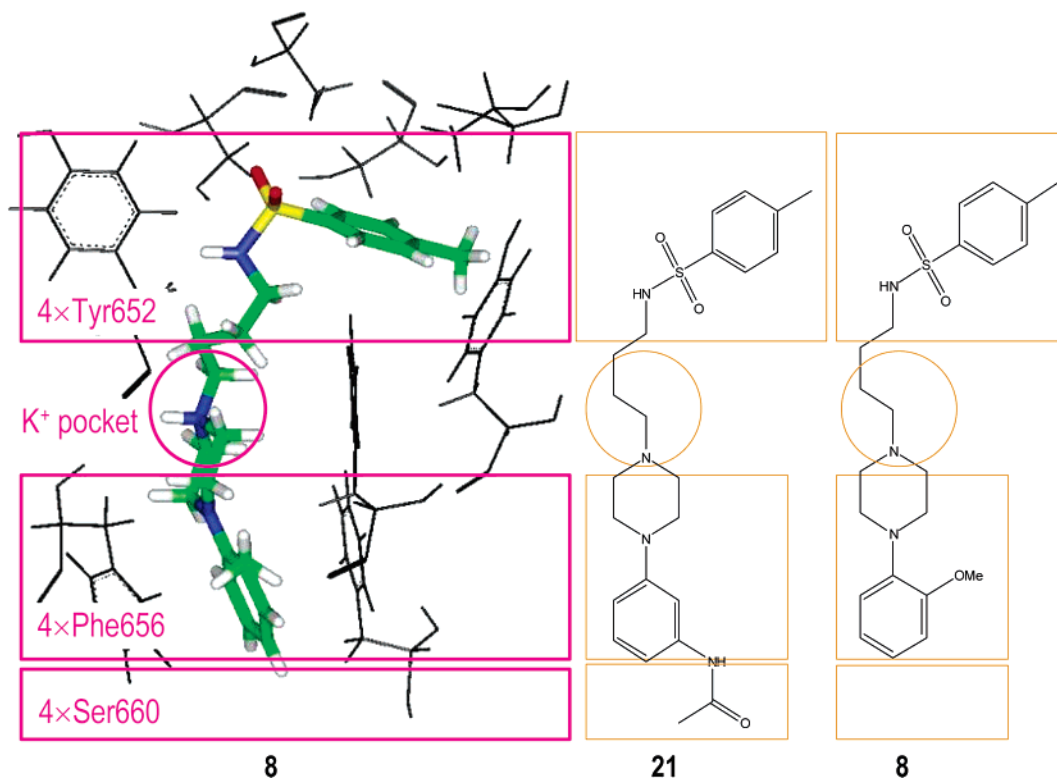


Figure 6. A comparison of the hERG binding modes of compounds **8** and **20d**. Shown are a detailed 3D view of the binding of compounds **8** in the hERG pore, as well as two schematic views of the binding of compounds **8** and **20d** next to each other. The four main interaction regions are highlighted in all views: An aromatic region formed by the four Tyr652 residues, a K⁺ pocket, an aromatic region formed by the four Phe656 residues, and a polar region formed by four Ser660 residues (shown only schematically). The greater hERG affinity of **20d** is probably due to its interaction with the Ser660 region. This interaction is not formed by compound **8**.

the hERG channel, the first step was to model its 3D structure based on the structure of a bacterial channel. The hERG K⁺ channel is composed of four identical subunits that coassemble to form a tetrameric structure. The basic secondary structure of each subunit is identical to that of other voltage-gated K⁺ channels subunits. Each monomer consists of six transmembrane segments (S1–S6), with large intracellular amino and carboxy-termini. The pore domain is formed by the S5–P–S6 segments, where P is a reentrant pore-forming linker that contains a helical K⁺ selectivity filter.⁵⁴ Because the closed KcsA ion channel (PDB code 1BL8)⁵⁵ that was used as a template for modeling the hERG channel (procedure described in the Experimental Section) has only two transmembrane domains, which are equivalent to the S5 and S6 domains of voltage-gated channels such as the hERG, the resulting 3D model is restricted to that channel forming portion of the tetramer. The channel pore structure was refined using a molecular-dynamics-based virtual complexation process with astemizole, a drug that was found to be an extremely potent hERG-channel blocker (IC₅₀ = 0.9 nM) causing QT-prolongation (astemizole was removed from the market in 1998 due to its potential hazards). Figure 5 depicts the 3D model of the hERG channel with astemizole bound to it (for more details, see Kalid, O et al., manuscript in preparation).

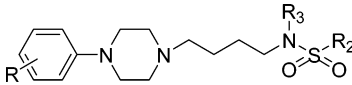
To develop an optimization strategy that would reduce hERG binding without compromising the affinity, selectivity, and PK goals that were already achieved in compound **20d**, it was necessary to understand why compound **20d** had 10-fold greater affinity to the hERG channel compared to the lead compound **8**. Figure 6 compares the binding modes of compounds **8** and **20d** in the hERG channel. As expected, both compounds adopt a similar binding-mode such that most of the interactions are identical for both compounds: the *p*-toluenesulfonyl group

interacts with Tyr652, the piperazine amine is located in the "K⁺ pocket", and the aryl group is sandwiched between two Phe656 residues. The only difference is that while the *m*-NHCOMe moiety of **20d** extends further and interacts also with residues Ser660, this additional interaction does not occur in the binding of **8**, which as an *o*-OMe moiety that points in a different direction. Interestingly, the potent hERG binder astemizole also has a moiety (*p*-OMe) that interacts with Ser660 (see Figure 5).

The structural analysis of the hERG binding mode of **20d** suggests that removing the H-bond capable group from the meta-position of **20d** should reduce hERG binding. However, this would also annul all of the previous optimization efforts. Namely, this analysis shows that the optimization strategy of Chart 2, which led to an efficient optimization of affinity, selectivity, and pharmacokinetics, is also the source of the increased affinity to the hERG channel. Since this was not a promising path, the conclusion was that the effort to reduce hERG affinity should focus on the other side of the compound, on the *p*-toluenesulfonyl region of **20d**. On the basis of the 3D model, the *p*-toluenesulfonyl group contributes to the hERG binding affinity of compound **20d** via interactions with the aromatic Tyr562 residues. Replacing the aromatic *p*-toluene (*p*-tol) substituent of **20d** with a nonaromatic hydrophobic group may offer an alternative strategy to reducing the hERG binding affinity. It should be noted that replacing the aromatic group by a nonaromatic group was not expected to remove hERG binding altogether, but it was hoped that it will reduce it enough to obtain the required selectivity window for the drug.

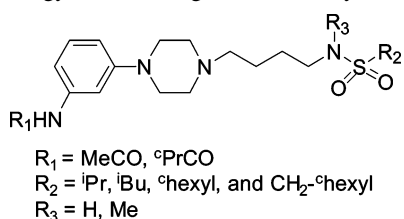
Fortunately, the structural analysis of the 5-HT_{1A} model also suggested that this modification should not have a significant effect on binding to the primary target. According to the 3D structure of 5-HT_{1A} (Figure 3a), there are no major aromatic

Table 3. Optimization of hERG Binding



compd	R	R ₂	R ₃	5-HT _{1A} : K _i (nM) ^a	α ₁ % ^b	α ₂ % ^b	hERG: IC ₅₀ nM (%) ^c
8	2-OMe	4-Me-Ph	H	1	6 nM	12 nM	>5000 (11%)
20d	3-MeCONH	4-Me-Ph	H	6.8	22	43	300 (73%)
20j	3-MeCONH	4-F-Ph	H	18	39	<10	
20k	3-MeCONH	^c hexyl	H	40	<10	<10	
20l	3-MeCONH	ⁱ Pr	H	24	<10	<10	
20m	3-MeCONH	CH ₂ - ^c hexyl	H	5.1	47	0	~3800 (21%)
20n	3- ^o PrCONH	CH ₂ - ^c hexyl	H	8.9	10	<10	~1500 (41%)
20o	3-MeCONH	ⁱ Bu	H	9.2	5	0	~3000 (25%)
20p	3-MeCONH	CH ₂ - ^c hexyl	Me	1.3	37	47	~4000 (20%)
20q	3-MeCONH	ⁱ Bu	Me	9.7	27	16	~2200 (31%)

^a K_i is the binding affinity determined using h5-HT_{1A} receptor expressed in HEK-293 cells using [³H]8-OH-DPAT as the radioligand (mean value; n = 2). ^b % displacement of the radioligand at 1 μM from the hα₁ and hα₂ adrenergic receptors in rat cerebral cortex cells using [³H]prazosin and [³H]RX 821002 as the radioligands, respectively (mean value; n = 2). ^c Estimated IC₅₀ (in nM) for inhibition of the hERG K⁺ current in a patch-clamp assay, based on measuring the % inhibition at 1 μM (mean value, n = 2, given in parentheses).

Chart 3. Strategy for Reducing hERG Affinity of **20d**

residues that interact with the *p*-toluenesulfonyl group, which is the nonpharmacophoric part of our compounds, suggesting that such a modification should not adversely impact binding to the 5-HT_{1A} target. Finally, this modification was also not expected to significantly increase the compound's affinity to α₁, since in the 3D structure of α₁ one finds an aromatic Phe residue in interaction with the *p*-toluene moiety (Figure 3b).

Hence, the structure-based strategy that was selected for reducing the hERG affinity of **20d** without affecting 5-HT_{1A} affinity and α₁ selectivity was to replace the *p*-toluene group with alicyclic and cyclic carbocycles such as isopropyl, isobutyl, cyclohexyl, and cyclohexylmethyl. Chart 3 describes this strategy, which led to the synthesis of compounds **20k–q**.

Table 3, which reports the SAR results for compounds **20j–q**, shows that the structure-based strategy of Chart 3 was proven to be very successful. All compounds in this series maintained excellent binding to the 5-HT_{1A} receptor as well as their selectivity toward α₁ while significantly reducing hERG binding by factors ranging from 5-fold to more than 10-fold, reducing hERG affinity from an IC₅₀ of 300 nM in **20d** to IC₅₀ values ranging from 1500 nM (**20n**) to 4000 nM (**20p**).

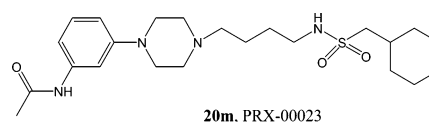
The cyclohexyl replacement of *p*-tol on the sulfonamide gave **20k** that had reduced hERG activity and slightly diminished binding affinity for 5-HT_{1A}. This compound, which is the closest analogue of the original *p*-tol in this series, also had lower affinity toward the α₁ and α₂ receptors, confirming the estimated role of the aromatic residue Phe193 in the binding of **20d** to α₁. The 5-HT_{1A} activity was improved by nearly 2-fold when reducing the size of the lipophilic cyclohexyl ring by replacing it with an isopropyl group to give compound **20l** (5-HT_{1A} K_i 24 nM). The lower K_i of **20k** and **20l** may be attributable to the shorter length and/or size of the cyclohexyl and isopropyl groups on the sulfonamide moiety. The size and the conformational constraint of the sulfonamides was optimized by incorporating cyclohexylmethylsulfonyl to yield **20m** which displayed improved 5-HT_{1A} activity (K_i 5.1 nM) while maintaining good selectivity. In hERG patch-clamp assay, **20m** was determined

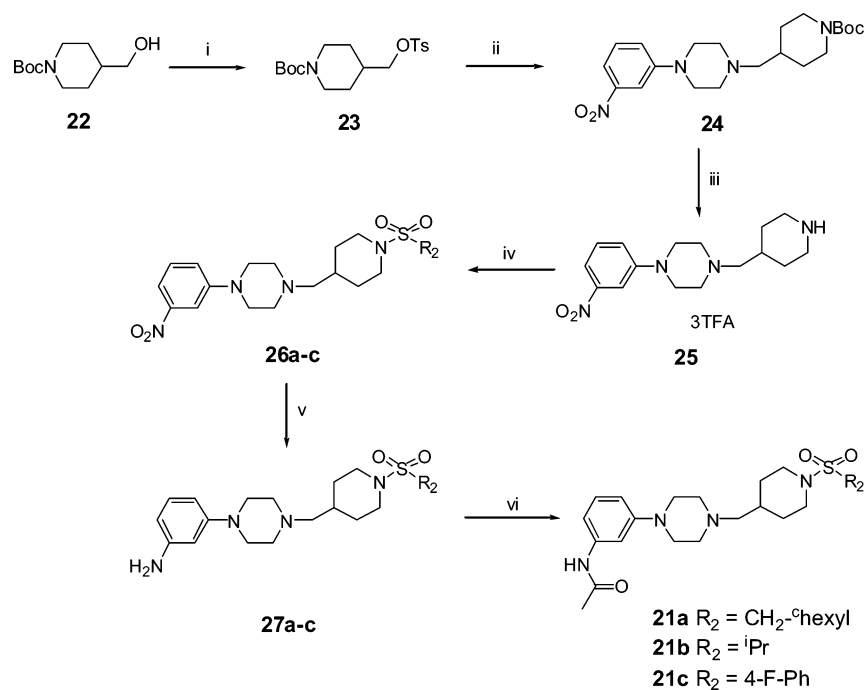
to be a weak hERG K⁺ channel blocker with low inhibitory potency of only 20% at 1 μM (estimated IC₅₀ 3800 nM). Since the cyclopropyl amide **20h** was found to be the most active (5-HT_{1A} K_i 22 nM) among all three propyl amide analogues (**20f**, **20g**, and **20h**) examined, a cyclopropyl amide compound **20n** was also designed and synthesized in which the terminal *p*-toluenesulfonamide group was replaced with an optimal cyclohexylmethyl moiety to improve target activity and selectivity. However, although the cyclopropyl amide **20n** showed good 5-HT_{1A} binding affinity (K_i = 8.9 nM) and even better selectivity than **20m**, its hERG K⁺ channel blocking affinity was too high, 41% at 1 μM (estimated IC₅₀ 1500 nM) not quite making the hERG selectivity target.

Replacement of the *p*-toluene (4-Me-Ph) sulfonyl with metabolically more stable 4-fluorophenylsulfonyl moiety yielded **20j** which has a nearly 3-fold reduced 5-HT_{1A} binding affinity (K_i = 18 nM) compared to **20m**, and was not pursued further.

Compound **20m** with 5-HT_{1A} K_i of 5.1 nM behaved as a full agonist in an in vitro cell-based functional assay with an EC₅₀ of 20 nM and showed excellent selectivity and pharmacokinetic profiles. Hence, **20m** was selected as the clinical candidate, and this compound is now in Phase III clinical trials for generalized anxiety disorder (GAD). A detailed report of the properties of **20m** and its analogues is given in the following section.

Note, that during the entire optimization process we did not change the length of the linker connecting the arylpiperazine to the sulfonamide. The reason is that a detailed in silico analysis of various linker lengths suggested that the four-carbon linker is already the optimal spacer. This is in full agreement with thorough SAR analysis on other arylpiperazine compounds which have demonstrated that the maximum affinity for both 5-HT_{1A} and α₁ receptors is reached with *n* = 3 or 4. Reduction to *n* = 2 or 1 leads to inactive or poorly active compounds.⁴³ Nonetheless, the computational analysis has suggested that making the linker more rigid may be beneficial. In particular it was suggested that replacing the linear *n*-butyl-sulfonamide linker with a 4-methylpiperidine-sulfonyl moiety would result in compounds that dock well into the 5-HT_{1A} binding site and thus will maintain, or even improve, the high affinity of corresponding linear compound. On the basis of this analysis, we prepared compounds **21a–c**. Compounds **21a–c** in Scheme



Scheme 2^a

^a Reagents: (i). Et₃N, CH₂Cl₂, TsCl, 90%; (ii) **11**, Et₃N, THF, 92%; (iii) TFA, CH₂Cl₂; (iv) R₂SO₂Cl, Et₃N, CH₂Cl₂, 90%; (v) SnCl₂, MeOH, HCl, 95%; (vi) CH₃COCl, Et₃N, CH₂Cl₂, 91%.

Table 4. Effect of Rigidifying the Linker

compd	R ₂	linker ^d	5-HT _{1A}			hERG
			K _i (nM) ^b	α ₁ , % ^c	α ₂ , % ^c	IC ₅₀ (nM) ^d
20m	CH ₂ - ^c hexyl	linear	5.1	47	0	~3800 (21%)
21a	CH ₂ - ^c hexyl	rigid	10	<10	13	~2000 (35%)
20l	ⁱ Pr	linear	24	<10	<10	
21b	ⁱ Pr	rigid	112	<10	<10	
20j	4-F-Ph	linear	18	39	<10	
21c	4-F-Ph	rigid	13	49	<10	

^a "linear" = *n*-butyl-sulfonamide ((CH₂)₄NH); "rigid" = 4-methylpiperidinesulfonyl. ^b K_i is the binding affinity determined using h5-HT_{1A} receptor expressed in HEK-293 cells using [³H]8-OH-DPAT as the radioligand (mean value; *n* = 2). ^c % displacement of the radioligand at 1 μM from the α₁ and α₂ adrenergic receptors in rat cerebral cortex cells using [³H]prazosin and [³H]RX 821002 as the radioligands, respectively (mean value; *n* = 2). ^d Estimated IC₅₀ (in nM) for inhibition of the hERG K⁺ current in a patch-clamp assay, based on measuring the % inhibition at 1 μM (mean value, *n* = 2, given in parentheses).

2 were synthesized by the same procedure as in method 2 of Scheme 1.

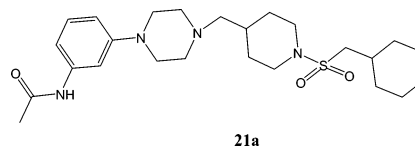
Table 4 shows the results for compounds **21a–c** in comparison to their linear counterparts, compounds **20m**, **20l**, and **20j**, respectively. The results show that two of the three rigid-linker compounds, **21a** and **21c**, maintained a 5-HT_{1A} affinity similar to that of their linear counterparts, in agreement with the computational prediction. Only compound **21b** was 4-fold less active compared to its linear linker counterpart **20l**, which in itself was the least active compound of the three linear compounds. Furthermore, rigidifying the linker also did not affect the affinity of the compounds to the α₁ and α₂ receptors, with the exception of **21a** which became even more selective toward α₁ relative to its linear counterpart **20m**. When tested for hERG binding compound **21a** showed 35% inhibition of the ion current at 1 μM (IC₅₀ ~ 2000 nM), which is within the

Table 5. Selectivity of **20m** or Serotonin Receptors

receptor	K _i	tissue
5-HT _{1A}	5.1–11 nM	human cDNA
5-HT _{1A}	17 nM	rat cerebral cortex
5-HT _{1B}	> 2 μM*	rat cerebral cortex
5-HT _{1D}	> 2 μM*	bovine
5-HT _{2A}	> 2 μM*	human cDNA
5-HT _{2B}	> 5 μM*	human
5-HT _{2C}	> 5 μM*	human
5-HT ₃	> 5 μM*	mouse
5-HT _{4e}	> 5 μM*	human
5-HT _{5A}	> 5 μM*	human cDNA
5-HT ₆	> 5 μM*	human
5-HT ₇	700 nM*	human cDNA

* *, Estimated based on % displacement at 1 μM.

200-fold 5-HT_{1A}/hERG selectivity target (5-HT_{1A} K_i = 10 nM). However, the pharmacokinetic properties of **21a** in rats showed that its methylpiperidine linker is being rapidly metabolized resulting in a very short 0.75 h serum half-life po, which is much shorter than the serum half-life of the linear linker compound **20m**.



Clinical Candidate. In Vitro Pharmacology. The development candidate **20m** (PRX-00023) demonstrates high affinity binding for the human and rat 5-HT_{1A} receptors (K_is of 5.1–11 nM and 17 nM, respectively) with more than a 400-fold difference in affinities for the 5-HT_{1A} receptor compared with all other 5-HT receptors (K_i > 2 μM, except for the 5-HT₇ with a K_i = 700 nM [Table 5]). **20m** was also devoid of binding to >50 additional proteins tested (K_i > 2 μM), including other neurotransmitters, other GPCRs, ion channels and transporters, including α- and β-adrenergics, dopamine, histamine, angiotensin II, benzodiazepines, bradykinins, endothelins, GABA,

Table 6. Pharmacological and Pharmacokinetic Data for Selected Compounds

assay	20m	20o	20q	20p	buspirone, 1
In Vitro Pharmacology ^a					
5-HT _{1A} K _i	5.1–11 nM	9.2 nM	9.7 nM	1.3 nM	20 nM
EC ₅₀	20 nM	60 nM	32 nM	3.6 nM	80 nM
α ₁ K _i	1600 nM	> 5000 nM	27% ^b	37% ^b	367 nM
D ₂ K _i	> 2000 nM	> 5000 nM			13 nM
hERG K _i	3800 nM	3000 nM	2200 nM	4000 nM	
hLM T _{1/2}	28 min	> 90 min	> 45 min	12 min	
hS9 T _{1/2}	65 min			65 min	
serum prot binding	92%	57%			
Cyp inhib	none	none			
In Vivo Pharmacokinetics ^c					
rat F%	11%	50%			< 1%
rat T _{1/2} po	2–3.5 h	3.5 h			1 h
rat C _{max} po	24 ng/mL	350 ng/mL			4 ng/mL
dog F%	16%	> 80%			9%
dog T _{1/2} po	1.1 h	2.4 h			1.0 h
dog C _{max} po	174 ng/mL	600 ng/mL			146 ng/mL
rat MTD po	600 mg/kg ^d	ND			< 200 mg/kg (LD ₅₀)
dog MTD po	600 mg/kg				< 600 mg/kg

^a For all in vitro pharmacology data shown is the mean value ($n \geq 2$). ^b % displacement of the radioligand from the α-1 adrenergic receptor at 10 μM. ^c Rat and dog pharmacokinetics determined following intravenous administration (1 mg/kg) and oral administration (3 mg/kg) (mean value, $n \geq 3$). ^d LD₁₀ could not be determined.

galanin, cholecystokinin, chemokines, melanocortins, muscarinics, neurokinins, neurotensin, orphanin, opioids, somatostatin, sigmas, vasoactive intestinal peptide, vasopressin, neuropeptides, and ion channels including Na⁺, K⁺, and Cl⁻, as well as transporters such as 5-HT, norepinephrine (NE), and dopamine (CEREP and MDS Pharma Services binding profiles; data not shown). The only receptor for which **20m** has significant affinity is the guinea pig sigma receptor ($K_i = 100$ nM). As reported above, in hERG patch-clamp assay, **20m** was determined to be a weak hERG K⁺ channel blocker with an estimated IC₅₀ of 3800 nM. Overall these data demonstrate that **20m** is a very selective ligand for the 5-HT_{1A} receptor. Compound **20m** was tested in functional cell-based assay, demonstrating that it has an EC₅₀ of 20 nM and behaves as a full agonist.

20m demonstrates a half-life ($t_{1/2}$) of 28 min in a human liver microsome (HLM) stability assay, which is three times greater than that of bupirone ($t_{1/2} = 9$ min), and a $t_{1/2}$ of 65 min in a human liver S9 fraction stability assay (without phase 2 cofactors), with 75% of the compound remaining after 15 min. **20m** does not inhibit cytochrome P450 isoforms (CYP) 1A2, 2C9, 2C19, 2D6, and 3A4. The major metabolites of **20m** were determined to be its mono-hydroxylated and deacetylated derivatives with 85% of **20m** remaining after 4 h in human hepatocytes. In a human serum protein binding assay, **20m** was found to be 92% protein bound at 2 μM and 10 μM, with the majority of this binding due to an interaction with α₁-acid glycoprotein.

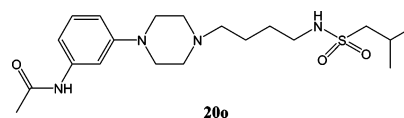
On the basis of the binding affinity, selectivity and functional potency, HLM stability, and other in vitro pharmacology parameters, **20m** was selected for further evaluation for efficacy in appropriate animal models, PK behavior in rats and dogs, and general safety. Some key properties of **20m** are listed in Table 6.

In Vivo Pharmacokinetics. A pharmacokinetic analysis of **20m** in both rats and dogs showed that the compound has a favorable PK profile. In rats **20m** shows 11% oral bioavailability with a serum $t_{1/2}$ of 2–3.5 h when administered po, attaining a C_{max} level of 24 ± 13 ng/mL (3 mg/kg, po). **20m** shows significant brain penetration, achieving a brain:serum concentration ratio of approximately 0.5 in the rat at 1 h following either intravenous or oral administration and reaching brain concentration approximately equivalent to that of bupirone. In dogs the

pharmacokinetic profile of **20m** shows 16% oral bioavailability, a serum $t_{1/2}$ of 1.1 h po, and a C_{max} level of 174 ± 141 ng/mL (3 mg/kg, po). This pharmacokinetics profile is far superior to that of bupirone **1** (Table 6). In rats bupirone exhibits less than 1% oral bioavailability and a 1 h serum $t_{1/2}$, reaching barely detectable maximal drug levels of 4 ng/mL (3 mg/kg, po). Bupirone does not have a significantly improved PK profile in dogs, in which the oral bioavailability is 9%, serum $t_{1/2}$ remains 1 h, although C_{max} levels reach 146 ± 10 ng/mL (3 mg/kg, po).

Namely, **20m** in vitro shows a half-life approximately 3 times longer than bupirone in human liver microsomes and human S9 liver fraction. In vivo, the serum $t_{1/2}$ is more than 3 times longer in rats and is similar to bupirone in dogs. Oral bioavailability of **20m** is superior to bupirone in both rats and dogs. Since bupirone requires three times daily (tid) dosing, these data suggest that **20m** may require only a single daily dose, a highly desirable property for any drug.

Backup Compounds. After identifying **20m** as the early development candidate, we continued to explore the strategy depicted in Chart 3 for the discovery of backup candidates. In compound **20o** the cyclohexylmethyl moiety of **20m** was replaced with an acyclic mimic, the isobutyl group. The isobutyl analogue **20o** showed excellent over all drug candidate profile



with high 5-HT_{1A} binding affinity ($K_i = 9.2$ nM) and higher selectivity than **20m** (Tables 3 and 5). The agonist activity EC₅₀ of **20o** in 5-HT_{1A} functional assay was determined to be 60 nM and its hERG binding IC₅₀ ~ 3000 nM, well within the target selectivity range. The half-life of **20o** in HLM assay was determined to be the longest of all compounds in the series with $t_{1/2}$ of >90 min which is attributable to its reduced lipophilicity and fewer number of sites available for enzymatic oxidative cleavage than that in **20m**. This metabolic stability was also observed in the cases of the N-Me analogue **20q** of compound **20o**, which was found to have a half-life >45 min in the HLM assay. Compound **20o** is only 57% protein bound and it does not inhibit CYPs 1A2, 2C9, 2C19, 2D6, and 3A4. Compound

20o also has a favorable PK profile, even better than that of **20m**. In rats compound **20o** shows 50% oral bioavailability, serum $t_{1/2}$ of 3.5 h po and C_{max} levels of 350 ng/mL, which are 7-fold higher than the corresponding levels of **20m**. In dogs compound **20o** shows >80% oral bioavailability, serum $t_{1/2}$ of 2.4 h po, and C_{max} levels of 600 ng/mL, which are 4-fold higher than the corresponding levels of **20m**. Compound **20o**, was selected as a backup to **20m**.

N-Methyl analogues, **20p** and **20q** of **20m** and **20o**, respectively, were designed to assess the effect of N-Me vs N-H of the sulfonamide on the biological activity. N-Me derivative **20p** of the cyclohexylmethylsulfonamide **20m** exhibited 4-fold increase in the 5-HT_{1A} binding affinity and slightly reduced selectivity than that of **20m** while the N-Me analogue **20q** of the isobutylsulfonamide **20o** was nearly equipotent in binding affinity and less selective than **20o** for the target 5-HT_{1A} receptor. Both N-methylated compounds **20p** and **20q** exhibited excellent agonist activity with EC₅₀ values of 3.6 nM and 32 nM, higher in both cases than their corresponding NH analogues **20m** and **20o**, respectively. The hERG inhibitory activity of **20p** and **20q** also met the target selectivity goal, estimated as 4000 nM, 2200 nM, 20% and 31% inhibition at 1 μ M in the patch-clamp assay, respectively. However, when tested in the HLM assay, it was found that both compounds were metabolized significantly faster than their corresponding N-H analogues (Table 6). Within the cyclohexylmethyl series **20p** has a HLM $t_{1/2}$ of 12 min compared to 28 min for **20m**, and within the isobutyl series **20q** has a HLM $t_{1/2}$ of >45 min compared to >90 min for **20o**. Overall, both compounds **20p** and **20q** have favorable profiles and could in principle also be considered as backup candidates.

In Vivo Efficacy. Compound **20m** was tested for anxiolytic efficacy in mice using the stress-induced hyperthermia model following oral administration of 1, 3, and 20 mg/kg doses of the compound. In addition, two doses of buspirone (3 and 20 mg/kg, ip) were included. The test is based upon the observation that an anxiogenic or stressful event will cause a rise in core body temperature in mammals.⁵⁶ Anxiolytics such as benzodiazepine receptor agonists (e.g., diazepam, chlordiazepoxide, alprazolam) and 5-HT_{1A} receptor agonists (e.g., buspirone) decrease the hyperthermic response to stress.⁵⁷

One hour after dosing, two rectal temperature measurements were obtained, basal temperature and, 10 min later, the body temperature due to the stress of the first rectal measurement. The difference (Delta T) in the two measurements reflects a stress-induced anxiogenic response. The procedure also measures the intrinsic activity of drugs on the basal body temperature, and Delta T is relatively independent from the intrinsic temperature effects of drugs.

Both **20m** and buspirone exerted a dose-dependent anxiolytic-like effect with a significant decrease in the hyperthermic response to stress (Delta T) at the 20 mg/kg dose (Figure 7). A significant reduction in basal rectal temperature was also seen at the high dose for both compounds (Figure 8).

Additional studies of **20m** have been performed using other anxiolytic assays such as the elevated plus maze and in animal models of attention-deficit hyperactivity disorder (ADHD). **20m** demonstrated significant efficacy in these studies, the results of which will be presented elsewhere.

Preclinical Safety. **20m** was subjected to a full range of preclinical safety and toxicology studies in two species. Both single and repeated dose studies indicated that the compound was well tolerated. As found with other 5-HT_{1A} agonists, increased prolactin levels were observed (in rats, this leads to

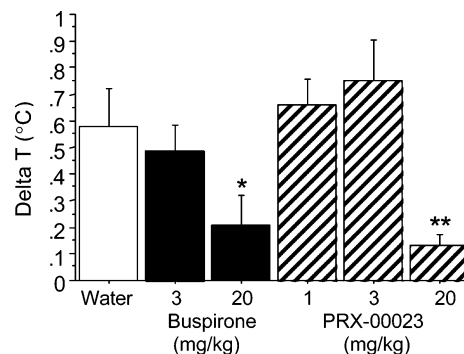


Figure 7. Effect of **20m** on Delta T (°C) in the stress-induced hyperthermia test. Seen are the increase in rectal temperature in vehicle-treated animals (stress-induced hyperthermia) and the blocking effect of buspirone (20 mg/kg; $P < 0.05$ vs vehicle-treated group) and **20m** (20 mg/kg; $P < 0.01$ vs vehicle-treated group). ANOVA revealed significant effect of Treatment ($p = 0.0009$). Follow-up Fisher's PLSD for paired comparison showed that buspirone (20 mg/kg) significantly decreased ($p = 0.024$) stress-induced hyperthermia. Similarly, **20m** in 20 mg/kg dose resulted in significant decrease ($p = 0.0067$). **20m** at 1 and 3 mg/kg did not show significant effects ($p = 0.618$ and $p = 0.2911$, respectively).

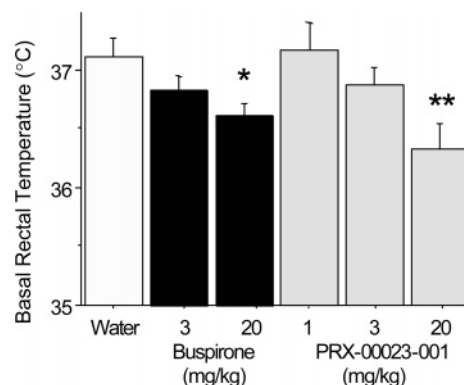


Figure 8. Effect of **20m** on basal rectal temperature (°C) in the stress-induced hyperthermia test. * $p < 0.05$, ** $p < 0.01$ vs vehicle-treated group (water). ANOVA revealed a significant effect of treatment ($p = 0.0109$). Follow-up Fisher's PLSD for paired comparison showed that **20m** (20 mg/kg) significantly decreased ($p = 0.0023$) basal rectal temperature. Similarly, buspirone in 20 mg/kg dose resulted in significant decrease ($p = 0.044$). Lower dose of **20m** (1 and 3 mg/kg) did not show significant effects ($p = 0.808$ and $p = 0.326$, respectively).

hyperprolactinemia effects at high doses). The maximum tolerated dose (MTD) of **20m** with a single oral administration was determined to be 300 and 600 mg/kg in rat and dog, respectively. The MTD values of **20m** exceed those of buspirone, which has an LD₅₀ of 196 mg/kg in rats and 586 mg/kg in dogs (Buspar package insert).

Clinical Development. On the basis of the desirable pharmacology, pharmacokinetics, animal efficacy, and toxicology results, **20m** was selected for clinical development for the treatment of anxiety and depression. Preclinical PK suggested that in humans **20m** could be dosed once- or twice-daily, and the negligible cross reactivity to other receptors, which was introduced into the compound through the rational structure-based optimization process, suggested that in humans **20m** should be well tolerated at efficacious doses.

To date, **20m** has completed three Phase I clinical trials in 84 healthy volunteers to evaluate the tolerability and pharmacokinetics of this drug at doses of 10 to 150 mg. In addition, a Phase II study has completed and the first of at least two pivotal Phase III clinical trials in patients with generalized anxiety disorder has been initiated.

A detailed review of **20m** clinical results is not within the scope of the present paper. Here we will only briefly report some key results which are important for comparison with the discovery effort and the preclinical data. **20m** was well tolerated at the expected efficacious doses while showing a desirable PK profile with a terminal half-life >10 h, superior to any azapirone tested so far, and supporting once-daily dosing. In a single-dose study, **20m** AUCs at all doses (10, 30, 40, and 60 mg) were substantially greater than buspirone AUC after a 30 mg buspirone dose. After single and multiple dosing, transient increases in serum prolactin levels were observed in response to **20m** at doses greater than 30 mg. Mean increases from baseline were approximately comparable to those seen with buspirone 30 mg, but the intrasubject variability was less with **20m** treatment.

The clinical experience with healthy volunteers receiving **20m** revealed no unexpected adverse events associated with treatment. **20m** was well tolerated in healthy volunteers in single doses up to 40 mg when administered in the fasting state. Headache and dizziness were observed in some subjects given a single dose of 60 mg after an overnight fast.

20m was also well tolerated when titrated up to doses of 150 mg daily in the multiple-dose studies when subjects initiated dosing at a dose level below 60 mg. There were no clinically meaningful changes observed in 12-lead electrocardiogram (ECG) intervals, clinical laboratory results, or vital signs.

Conclusion

In conclusion, using an in silico model-driven and structure-based approach we have discovered a novel series of potent and selective acylaminophenylpiperazinyl sulfonamide-based 5-HT_{1A} agonists that exhibit the desired oral bioavailability, safety, and efficacy in preclinical animal studies. On the basis of in vitro and in vivo potency, efficacy, and pharmacokinetic characteristics, **20m**, *N*-(3-(4-(4-(cyclohexylmethylsulfonamido)-butyl)piperazin-1-yl)phenyl)acetamide, was chosen as the clinical development candidate and **20o**, *N*-(3-(4-(4-(2-methylpropylsulfonamido)butyl)piperazin-1-yl)phenyl)acetamide, was selected as the back-up candidate for the treatment of anxiety, depression, and ADHD.

In Phase I human clinical trials, **20m** (once daily and 28 day multiple doses up to 60 mg) was well tolerated showing an excellent side-effect profile with no effect on cardiovascular or electrocardiographic parameters, as expected from a selective 5-HT_{1A} receptor agonist.

It is important to note that the favorable clinical properties of **20m** that were seen in the Phase I clinical studies—tolerability, pharmacokinetics, and pharmacodynamics—can be directly attributed to the structure-based optimization process described in this paper:

•**Tolerability:** **20m** is the product of a structure-based in silico-driven optimization process that rationally and efficiently minimized cross-reactivity to other receptors including α_1 -adrenergic receptor (α_1 -AR), α_2 -AR, and the hERG K⁺ channel, leading to a potent, selective, full agonist of 5-HT_{1A}. This in vitro selectivity profile correlates well with the favorable clinical safety and tolerability profile of **20m**, as observed in 84 healthy volunteers in three Phase I studies.

•**Pharmacokinetics:** The pharmacokinetic profile of the target compound was one of the most important parameters in the optimization process, leading to **20m** which shows a preclinical PK profile with a serum half-life approximately 3 times longer than, and oral bioavailability superior to, buspirone. This preclinical profile translated to an excellent PK profile in

the human Phase I studies, with good absorption and a terminal half-life >10 h supporting a once daily dosing. Namely, **20m** shows promise as a once-daily alternative to other 5-HT_{1A} agonists such as buspirone (Buspar), which require three times daily (tid) dosing.

•**Pharmacodynamics:** **20m** is a potent full agonist of 5-HT_{1A} with EC₅₀ levels of 20 nM in cell-based assays. The drug showed activity in animal models of anxiety and ADHD. While discussion of **20m** human efficacy is not within the scope of this paper, we have reported response of a known surrogate marker for 5-HT_{1A} efficacy (transient prolactin levels) both in the in vivo animal studies and in healthy volunteers in the Phase I studies. The efficacy of **20m** was suggested in the Phase II study that was completed, leading to the current ongoing Phase III study in generalized anxiety disorder.

As described above, the lead optimization process that led from the lead compound **8** to the clinical candidate **20m** and its backup candidate **20o** was in silico-driven, adopting a structure-based approach which relied on in silico generated 3D models of the target receptors. The total number of compounds synthesized in this project was only 31 compounds, representing approximately 10% of the number of virtual compounds that were computationally evaluated during the optimization process. The whole optimization process took less than 6 months from start to end, engaging only three medicinal chemists working together with two to three computational chemists fully dedicated to the project. This 1:1 ratio of medicinal to computational chemists is a key aspect of the drug discovery paradigm developed at Predix. This team structure is essential for enabling a thorough in silico analysis of each suggested compound, which leads to focused prioritization of compound synthesis that in turn translates to a more efficient drug discovery process. The discovery and optimization processes detailed here have culminated in a safe and tolerable drug candidate with a desirable PK profile that is undergoing a Phase III study in GAD, all within 30 months.

Experimental Section

•**GPCR Modeling.** The PREDICT algorithm^{45–47} searches through the receptors' conformational space for the most stable 3D structure(s) of the transmembrane (TM) domain of the GPCR protein within the membrane environment. To ensure that the final model represents the most stable conformation, the method simultaneously optimizes several thousand alternative conformations of the receptor. Following two successive application of the PREDICT algorithm (coarse modeling followed by fine modeling), the resulting model is subjected to molecular dynamics refinement using CHARMM⁵⁸ and the CHARMM22 force field.⁵⁹ Multiple constraints are applied during the simulations to ensure that the model does not deviate significantly from the initial PREDICT model. These refinement dynamics introduce helical kinks and relax the side chain conformations. Finally, a protein–ligand complex is carefully constructed through molecular dynamics.

The 3D model of the 5-HT_{1A} receptor and the α_1 receptor was modeled by the PREDICT program, following the procedure that was reported in detail in refs 45–47. Briefly, following two successive application of the PREDICT algorithm (coarse modeling followed by fine modeling), the resulting model was subjected to molecular dynamics refinement using CHARMM⁵⁸ and the CHARMM22 force field.⁵⁹ Multiple constraints were applied during the simulations to ensure that the model does not deviate significantly from the initial PREDICT model. Finally, a protein–ligand complex is carefully constructed through molecular dynamics.

•**Screening Library.** The screening library consists of virtual 2D representations of approximately 2 100 000 drug-like compounds, obtained from electronic catalogs of more than 20 vendors worldwide. The library is updated quarterly, so that at any given

time, it represents compounds that can be purchased on short notice. The multiple sources of the library ensure its diversity, allowing us to explore broad chemical spaces.

Library Preparation. The virtual compound library is processed prior to docking. This step includes 2D to 3D conversion (using CONCORD),⁶⁰ assignment of Gasteiger atom types,⁶¹ assignment of atomic charges, identification of multiple anchors for docking (using HYPERION software from Predix), generating multiple conformations for these anchors (using CONFORT),⁶² and more. Approximately 10% of the full library (on the order of 150 000 compounds) is selected for screening, according to the character of the binding site (charges, polar, or hydrophobic), and to the desired range of molecular weights, compound diversity, drug-like properties, etc.

In Silico Screening. The screening library was docked into the binding site using the DOCK4.0.^{63,64} Docking for each compound (often represented by five or more different anchor conformations) is repeated 10 times. The specific docking parameters are fine-tuned for each target separately, by optimizing the docking of a small set of known binders (if available) relative to a large drug-like random compound library.

Scoring and Selection. A sequential application of several scoring tools and selection criteria is used, until a list of fewer than 100 virtual hits is reached (Marantz et al, manuscript in preparation). First, an automated binding-mode analysis (using the Predix program BMA) is performed on all docked conformations to ensure proper docking. Ten additional 3D scores are calculated for the top 10% of the library based on the best DOCK scores that pass BMA (using DOCK,⁶⁴ CSCORE,⁶⁵ and CHARMM⁵⁸). Specific score cutoff values or combination cutoff values are used to further narrow the list of virtual hits. Finally, the remaining compounds in the hit list are clustered, with only the best-scored representative(s) of the similarity cluster selected for in vitro testing.

Modeling the hERG Ion Channel. The S5–S6 region of the hERG channel was modeled using the structure of the closed KcsA ion channel (PDB code 1BL8),⁵⁵ which only two transmembrane domains, as a template. The sequence alignment between the pore regions of KcsA (residues 43–119) and hERG (residues 572–668) was based on the partial alignment published by Doyle *et al.*⁵⁵ and previously utilized by Mitcheson *et al.*⁵⁴ Initially, all KcsA residues without identical hERG counterparts were manually mutated to fit the hERG sequence using the Sybyl Biopolymer module (version 6.8; Tripos Inc.: St. Louis, MO). This process distorted the structure of some proline residues, which were subsequently fixed with the “Fix Proline” function in the same Sybyl module. The structure was then energy-minimized with a fixed backbone constraint using the Tripos force field and the Powell minimization algorithm set to terminate at an energy gradient of 0.01 kcal/(mol·Å²). Following minimization, all rotamers were optimized using the “rotamer optimization” function in the InsightII Biopolymer module (Release 2000.1; Accelrys Inc., San Diego, CA).

The channel pore structure was further refined using a molecular-dynamics-based virtual complexation process with astemizole (Hismanal), a drug that was found to be an extremely potent hERG-channel blocker (IC₅₀ = 0.9 nM) causing QT-prolongation (astemizole was removed from the market in 1998 due to its potential hazards). Astemizole was manually docked into the channel pore region of the hERG model using InsightII. Molecular dynamics simulations were performed using CHARMM⁵⁸ and the CFF force field,⁶⁶ following a procedure described in detail elsewhere, where a detailed analysis of the model can also be found (Kalid O. *et al.*, manuscript in preparation).

Chemistry. All reagents used were obtained from commercially available sources. Solvents used in reaction were purchased from Sigma-Aldrich and Alfa Aesar while solvents for chromatography were obtained from VWR. ¹H nuclear magnetic resonance (NMR) spectra were recorded at 400 MHz on a Varian AS400 spectrometer and referenced to the NMR solvent. Chemical shifts were reported in parts per million (ppm, δ) relative to an internal standard (tetramethylsilane) with coupling constants given in hertz (Hz, J). ¹H NMR multiplicity data are denoted by s (singlet), d (doublet),

t (triplet), q (quartet), m (multiplet), and sb (singlet broad). Flash chromatography was performed in columns of various diameters with Merck silica gel (230–400 mesh) by elution with solvent systems indicated in the parentheses. Positive electrospray ionization (ESI) mass spectra were determined on a Finnigan LAD00416 mass spectrometer. Elemental analyses were carried out by Atlantic Microlab, Inc., and were within $\pm 0.4\%$ of the theoretical value. Melting points were performed on a Mettler-Toledo FP62 instrument. The instrument uses optical detection when determining the sample melting point.

1-(3-Nitro-phenyl)-piperazine (11). A mixture of 3-nitro-phenylamine (**10**) (13.8 g, 0.1 mol), bis-(2-chloro-ethyl)-amine hydrochloride salt (17.5 g, 0.1 mol), and potassium carbonate (48.3 g, 0.35 mol) in chlorobenzene (300 mL) was refluxed for 48 h. The mixture was poured into water (300 mL). The organic layer was separated, and the water phase was extracted with dichloromethane (3 \times 150 mL). The combined organic phases was dried over sodium carbonate, filtered, concentrated under pressure, and purified with flash chromatography on silica gel (eluent 2% MeOH in CH₂Cl₂) to give 9.3 g of the titled compound **11** (45% yield). ¹H NMR (CDCl₃): δ 7.71 (s, 1H), 7.65 (d, J = 8.0 Hz, 1H), 7.39–7.35 (m, 1H), 7.19 (d, J = 8.4 Hz, 1H), 3.25–3.23 (m, 4H), 3.07–3.04 (m, 4H), 1.68 (s, 1H); MS (ESI): m/z 208 (M + H)⁺.

Toluene-4-sulfonic Acid 4-(Toluene-4-sulfonylamino)-butyl Ester (13a). To an ice-cooled solution of 4-amino-butan-1-ol (**12a**) (1.0 g, 11.0 mmol) in anhydrous methylene chloride (25 mL) under N₂ was added Et₃N (6.1 mL, 44.0 mmol), followed by tosyl chloride (4.6 g, 24.2 mmol). The mixture was stirred at 0 °C for 3 h and then quenched with cold aqueous saturated NaHCO₃ solution (25 mL), and the organic phase was washed with water (3 \times 25 mL), dried over Na₂SO₄, and filtered. Solvent was removed under reduced pressure to give a brownish-red residue. The crude material was used for next step without further purification. MS (ESI): m/z 398 (M + H)⁺.

4-Methyl-N-{4-[4-(3-nitro-phenyl)-piperazin-1-yl]-butyl}-benzenesulfonamide (18a). A mixture of 1-(3-nitro-phenyl)-piperazine (**11**) (2.07 g, 10 mmol), **13a** (3.93 g, 10 mmol), and triethylamine (2.02 g, 20 mmol) in THF (100 mL) was stirred under nitrogen at ambient temperature for 48 h. The reaction mixture was diluted with dichloromethane, washed with 10% aqueous sodium carbonate solution (2 \times 100 mL) and water (2 \times 100 mL), and dried over sodium sulfate. After removal of sodium sulfate, solvent was evaporated under reduced pressure. The residue was purified by flash chromatography on silica gel (eluent 2% MeOH in CH₂Cl₂) to give 3.3 g (76% yield) of the title compound as a white solid. ¹H NMR (CDCl₃): δ 7.74 7.66 (m, 4H), 7.40 (t, J = 8.4 Hz, 1H), 7.29 (d, J = 7.6 Hz, 2H), 7.22–7.20 (m, 1H), 3.34–3.2 (m, 4H), 2.99 (t, J = 4.4 Hz, 1H), 2.63–2.61 (m, 4H), 2.42 (s, 3H), 2.39 (t, J = 5.6 Hz, 2H), 1.61–1.59 (m, 4H); MS (ESI): m/z 433 (M + H)⁺.

N-(3-{4-[4-(Toluene-4-sulfonylamino)-butyl]-piperazin-1-yl}-phenyl)-acetamide (9). This compound (as a colorless oil-like liquid) was prepared by using 1-phenyl-piperazine and **12a** in the same manner as compound **18a**, described above, and was purified by silica gel chromatography (eluent 1% MeOH in CH₂Cl₂) (97% yield); ¹H NMR (CDCl₃): δ 7.96 (d, J = 8.0 Hz, 2H), 7.60 (d, J = 7.6 Hz, 1H), 7.46–7.42 (m, 3H), 7.04 (d, J = 8.0 Hz, 1H), 6.90–6.86 (m, 1H), 3.35–3.30 (m, 4H), 3.06–3.02 (m, 2H), 2.70–2.66 (m, 4H), 2.46 (s, 3H), 2.42 (t, J = 5.4 Hz, 2H), 2.28 (s, 3H), 1.62–1.66 (m, 4H); MS (ESI): m/z 445 (M + H)⁺. Anal. (C₂₁H₂₉N₃O₂S) C, H, N.

N-{4-[4-(3-Amino-phenyl)-piperazin-1-yl]-butyl}-4-methylbenzenesulfonamide (19a). To a solution of tin chloride (3.5 g, 18.5 mmol) in methanol (50 mL) and concentrated hydrochloric acid (10 mL) was added a solution of **18a** (800 mg, 1.85 mmol) in methanol (50 mL) in one portion at –10 °C. The reaction mixture was allowed to warm to ambient temperature and stirred until the reaction was completed as determined by TLC. The reaction was quenched by adding 10% sodium carbonate solution (200 mL) and extracted with dichloromethane (3 \times 200 mL). The combined extracts were dried over sodium sulfate and evaporated under

reduced pressure. The residue was separated by flash chromatography on silica gel (eluent 2% MeOH in CH₂Cl₂) to give the titled compound (670 mg, 90% yield). ¹H NMR (CDCl₃): δ 7.75 (d, *J* = 8.4 Hz, 2H), 7.29 (d, *J* = 8.4 Hz, 2H), 7.09 (t, *J* = 8.0 Hz, 1H), 6.41 (d, *J* = 8.0 Hz, 1H), 6.30 (s, 1H), 6.28 (d, *J* = 8.0 Hz, 1H), 3.65 (sb, 2H), 3.25–3.22 (m, 4H), 3.00 (t, *J* = 5.6 Hz, 2H), 2.63–2.61 (m, 4H), 2.45 (s, 3H), 2.41 (t, *J* = 5.6 Hz, 2H), 1.64–1.60 (m, 4H); MS (ESI): *m/z* 403 (M + H)⁺.

***N*-{4-[4-(3-Methanesulfonylamino-phenyl)-piperazin-1-yl]-butyl}-4-methyl-benzenesulfonamide (20a).** To a mixture of compound **19a** (31 mg, 0.077 mmol) and triethylamine (0.5 mL) in dichloromethane (5 mL) was added methanesulfonyl chloride (0.008 mL, 0.10 mmol) at 0 °C. The mixture was stirred at ambient temperature for 30 min and concentrated on vacuum to dryness. The resulting residue was diluted with dichloromethane, washed with aqueous sodium carbonate solution and water, dried over sodium sulfate, filtered, and concentrated. Purification by silica gel chromatography (eluent 1% MeOH in CH₂Cl₂) gave 36 mg (97%) of the desired product **14** as a white solid. ¹H NMR (CDCl₃): δ 7.71 (d, *J* = 8.0 Hz, 2H), 7.27 (d, *J* = 8.0 Hz, 2H), 7.24–7.20 (m, 1H), 6.81 (s, 1H), 6.74 (d, *J* = 7.6 Hz, 1H), 6.67 (d, *J* = 7.4 Hz, 1H), 3.28–3.22 (m, 4H), 3.01 (s, 3H), 2.96 (t, *J* = 5.6 Hz, 2H), 2.62–2.58 (m, 4H), 2.41 (s, 3H), 2.37 (t, *J* = 6.0 Hz, 2H), 1.61–1.57 (m, 4H); MS (ESI): *m/z* 481 (M + H)⁺. Anal. (C₂₂H₃₂N₄O₄S₂) C, H, N.

***N*-{4-[4-(3-Ethanesulfonylamino-phenyl)-piperazin-1-yl]-butyl}-4-methyl-benzenesulfonamide (20b).** This compound (as a white solid) was prepared by using **19a** and ethanesulfonyl chloride in the same manner as compound **20a**, described above, and was purified by silica gel chromatography (eluent 1% MeOH in CH₂Cl₂) (98% yield); ¹H NMR (CDCl₃): δ 7.72 (d, *J* = 8.0 Hz, 2H), 7.29 (d, *J* = 8.0 Hz, 2H), 7.24–7.20 (m, 1H), 6.85–6.81 (m, 1H), 6.74 (d, *J* = 7.6 Hz, 1H), 6.64 (d, *J* = 7.4 Hz, 1H), 3.32–3.28 (m, 4H), 3.16–3.12 (m, 2H), 2.98–2.86 (m, 2H), 2.69–2.66 (m, 4H), 2.48–2.44 (m, 2H), 2.42 (s, 3H), 1.64–1.60 (m, 4H), 1.39–1.35 (m, 3H); MS (ESI): *m/z* 495 (M + H)⁺. Anal. (C₂₃H₃₄N₄O₄S₂) C, H, N.

4-Methyl-*N*-(4-[4-[3-(propane-2-sulfonylamino)-phenyl]-piperazin-1-yl]-butyl)-benzenesulfonamide (20c). This compound (as a white solid) was prepared by using **19a** and propane-2-sulfonyl chloride in the same manner as compound **20a**, described above, and was purified by silica gel chromatography (eluent 1% MeOH in CH₂Cl₂) (93% yield); ¹H NMR (CDCl₃): δ 7.72 (d, *J* = 8.0 Hz, 2H), 7.26 (d, *J* = 8.0 Hz, 2H), 7.20–7.16 (m, 1H), 6.85–6.84 (m, 1H), 6.71–6.67 (m, 2H), 3.36–3.30 (m, 1H), 3.24–3.22 (m, 4H), 2.96 (t, *J* = 5.4 Hz, 2H), 2.59–2.56 (m, 4H), 2.41 (s, 3H), 2.36 (t, *J* = 5.2 Hz, 2H), 1.58–1.56 (m, 4H), 1.38 (d, *J* = 6.8 Hz, 6H); MS (ESI): *m/z* 509 (M + H)⁺. Anal. (C₂₄H₃₆N₄O₄S₂) C, H, N.

***N*-{3-[4-[4-(Toluene-4-sulfonylamino)-butyl]-piperazin-1-yl]-phenyl}-acetamide (20d).** This compound (as a white solid) was prepared by using **19a** and acetyl chloride in the same manner as compound **20a**, described above, and was purified by silica gel chromatography (eluent 1% MeOH in CH₂Cl₂) (97% yield); ¹H NMR (CDCl₃): δ 7.96 (d, *J* = 8.0 Hz, 2H), 7.60 (d, *J* = 7.6 Hz, 1H), 7.46–7.42 (m, 3H), 7.04 (d, *J* = 8.0 Hz, 1H), 6.90–6.86 (m, 1H), 3.35–3.30 (m, 4H), 3.06–3.02 (m, 2H), 2.70–2.66 (m, 4H), 2.46 (s, 3H), 2.42 (t, *J* = 5.4 Hz, 2H), 2.28 (s, 3H), 1.62–1.66 (m, 4H); MS (ESI): *m/z* 445 (M + H)⁺. Anal. (C₂₃H₃₂N₄O₃S) C, H, N.

***N*-{3-[4-[4-(Toluene-4-sulfonylamino)-butyl]-piperazin-1-yl]-phenyl}-propionamide (20e).** This compound (as a white solid) was prepared by using **19a** and propionyl chloride in the same manner as compound **20a**, described above, and was purified by silica gel chromatography (eluent 1% MeOH in CH₂Cl₂) (97% yield); ¹H NMR (CDCl₃): δ 8.30 (s, 1H), 7.72 (d, *J* = 8.0 Hz, 2H), 7.40 (s, 1H), 7.32 (m, 3H), 6.84 (d, *J* = 7.6 Hz, 1H), 6.62 (d, *J* = 7.4 Hz, 1H), 3.24–3.22 (m, 4H), 2.94 (t, *J* = 5.6 Hz, 2H), 2.64–2.60 (m, 4H), 2.40 (s, 3H), 2.38 (m, 4H), 1.59 (m, 4H), 1.24 (t, *J* = 6.8 Hz, 3H); MS (ESI): *m/z* 459 (M + H)⁺. Anal. (C₂₄H₃₄N₄O₃S) C, H, N.

***N*-{3-[4-[4-(Toluene-4-sulfonylamino)-butyl]-piperazin-1-yl]-phenyl}-butyramide (20f).** This compound (as a white solid) was prepared by using **19a** and butyryl chloride in the same manner as compound **20a**, described above, and was purified by silica gel chromatography (eluent 1% MeOH in CH₂Cl₂) (91% yield); ¹H NMR (CDCl₃): δ 7.70 (d, *J* = 8.0 Hz, 2H), 7.36 (s, 1H), 7.27–7.16 (m, 4H), 6.87 (d, *J* = 7.6 Hz, 1H), 6.66 (d, *J* = 8.4 Hz, 1H), 3.24–3.22 (m, 4H), 2.97–2.95 (m, 1H), 2.58–2.56 (m, 4H), 2.40 (s, 3H), 2.37–2.32 (m, 4H), 1.79–1.73 (m, 2H), 1.58–1.57 (m, 4H), 1.01 (t, *J* = 7.6 Hz, 3H). MS (ESI): *m/z* 473 (M + H)⁺. Anal. (C₂₅H₃₆N₄O₃S) C, H, N.

***N*-{3-[4-[4-(Toluene-4-sulfonylamino)-butyl]-piperazin-1-yl]-phenyl}-isobutyramide (20g).** This compound (as a white solid) was prepared by using **19a** and isobutyryl chloride in the same manner as compound **20a**, described above, and was purified by silica gel chromatography (eluent 1% MeOH in CH₂Cl₂) (92% yield); ¹H NMR (CDCl₃): δ 7.71 (d, 2H, *J* = 8.4 Hz), 7.44 (m, 1H), 7.25–7.12 (m, 3H), 6.84–6.82 (m, 1H), 6.68–6.65 (m, 1H), 3.27–3.26 (m, 4H), 2.98–2.95 (m, 1H), 2.61–2.58 (m, 4H), 2.553–2.49 (m, 1H), 2.41 (s, 3H), 2.40–2.38 (m, 2H), 1.60–1.58 (m, 4H), 1.27 (s, 3H), 1.26 (s, 3H). MS (ESI): *m/z* 473 (M + H)⁺. Anal. (C₂₅H₃₆N₄O₃S) C, H, N.

Cyclopropanecarboxylic Acid (3-[4-[4-(Toluene-4-sulfonylamino)-butyl]-piperazin-1-yl]-phenyl)-amide (20h). This compound (as a white solid) was prepared by using **19a** and cyclopropanecarbonyl chloride in the same manner as compound **20a**, described above, and was purified by silica gel chromatography (eluent 1% MeOH in CH₂Cl₂) (75% yield); ¹H NMR (CDCl₃): δ 7.70 (d, *J* = 8.0 Hz, 2H), 7.42–7.40 (m, 2H), 7.26–7.16 (m, 2H), 6.83 (d, *J* = 7.6 Hz, 1H), 6.65 (d, *J* = 8.0 Hz, 1H), 3.24–3.22 (m, 4H), 2.96 (t, *J* = 5.2 Hz, 2H), 2.59–2.567 (m, 4H), 2.40 (s, 3H), 2.37 (m, 2H), 1.60–1.48 (m, 5H), 1.09–1.07 (m, 2H), 0.86–0.83 (m, 2H). MS (ESI): *m/z* 471 (M + H)⁺. Anal. (C₂₅H₃₄N₄O₃S) C, H, N.

***N*-{3-(4-(4-(Tosylamino)butyl)piperazin-1-yl)phenyl}pivalamide (20i).** This compound (as a white solid) was prepared by using **19a** and pivaloyl chloride in the same manner as compound **20a**, described above, and was purified by silica gel chromatography (eluent 1% MeOH in CH₂Cl₂) (85% yield); ¹H NMR (CDCl₃): δ 7.71 (d, *J* = 7.6 Hz, 2H), 7.44–7.35 (m, 1H), 7.29–7.26 (m, 3H), 7.19 (t, *J* = 8.4 Hz, 1H), 6.82 (d, *J* = 8.0 Hz, 1H), 6.67 (d, *J* = 8.4 Hz, 1H), 3.25 (m, 4H), 2.96 (t, *J* = 5.2 Hz, 2H), 2.60–2.56 (m, 4H), 2.40 (s, 3H), 2.36 (t, *J* = 5.2 Hz, 2H), 1.59–1.58 (m, 4H), 1.32 (s, 9H); MS (ESI): *m/z* 487 (M + H)⁺. Anal. (C₂₆H₃₈N₄O₃S) C, H, N.

4-Fluoro-benzenesulfonic Acid 4-(4-Fluoro-benzenesulfonylamino)-butyl Ester (13b). This compound was prepared by using **12a** and 4-fluorobenzene-1-sulfonyl chloride in the same manner as compound **13a**, described above, and was used for next step without further purification. MS (ESI): *m/z* 406 (M + H)⁺.

4-Fluoro-*N*-{4-[4-(3-nitro-phenyl)-piperazin-1-yl]-butyl}-benzenesulfonamide (18b). This compound was prepared by using **11** and **13b** in the same manner as compound **18a**, described above, and was purified by silica gel chromatography (eluent 2% MeOH in CH₂Cl₂) (75% yield). ¹H NMR (CDCl₃): δ 7.85 (m, 2H), 7.75–7.63 (m, 2H), 7.22–7.06 (m, 4H), 3.39–3.37 (m, 4H), 2.97–2.95 (m, 2H), 2.45–2.43 (m, 4H), 2.05–2.03 (m, 1H), 1.61–1.63 (m, 4H); MS (ESI): *m/z* 437 (M + H)⁺.

4-Fluoro-*N*-{4-[4-(3-amino-phenyl)-piperazin-1-yl]-butyl}-benzenesulfonamide (19b). This compound was prepared by reducing **18b** in the same manner as compound **19a**, described above, and was purified by silica gel chromatography (eluent 2% MeOH in CH₂Cl₂) (yield 87%); ¹H NMR (CDCl₃): δ 7.95 (m, 2H), 7.45–6.95 (m, 4H), 6.51–6.19 (m, 2H), 3.95–3.45 (m, 4H), 3.12–2.83 (m, 4H), 2.65–2.31 (m, 7H), 1.61 (m, 4H); MS (ESI): *m/z* 407 (M + H)⁺.

***N*-{3-[4-[4-(4-Fluoro-benzenesulfonylamino)-butyl]-piperazin-1-yl]-phenyl}-acetamide (20j).** This compound (as a white solid) was prepared by using **19b** and acetyl chloride in the same manner as compound **20a**, described above, and was purified by silica gel chromatography (eluent 1% MeOH in CH₂Cl₂) (95% yield); ¹H

NMR (CDCl₃): δ 7.45–7.16 (m, 4H), 6.81 (d, J = 8.9 Hz, 2H), 6.65 (d, J = 8.9 Hz, 2H), 3.48 (s, 1H), 3.28 (m, 4H), 2.95 (m, 2H), 2.62 (m, 5H), 2.35 (m, 2H), 2.08 (s, 3H), 1.65 (m, 4H); MS (ESI): m/z 449 (M + H)⁺. Anal. (C₂₂H₂₉FN₄O₃S) C, H, N.

Cyclohexyl-methanesulfonic Acid 4-(Cyclohexylmethanesulfonyl-methyl-amino)-butyl Ester (13c). This compound was prepared by using 4-(methylamino)butan-1-ol (**12b**) and cyclohexylmethanesulfonyl chloride in the same manner as compound **13a**, described above, and was used for next step without further purification. ¹H NMR (CDCl₃): δ 4.23 (m, 4H), 3.29 (t, J = 6.7 Hz, 4H), 3.00–2.61 (m, 8H), 2.27 (s, 3H), 1.99–1.45 (m, 18H); MS (ESI): m/z 424 (M + H)⁺.

C-Cyclohexyl-N-methyl-N-{4-[4-(3-nitro-phenyl)-piperazin-1-yl]-butyl}-methanesulfonamide (18c). This compound was prepared by using **11** and **13c** in the same manner as compound **18a**, described above, and was purified by silica gel chromatography (eluent 1% MeOH in CH₂Cl₂) (71% yield). ¹H NMR (CDCl₃): δ 7.35 (s, 1H), 7.23 (t, J = 7.3 Hz, 1H), 6.94 (d, J = 6.9 Hz, 1H), 6.81 (d, J = 7.4 Hz, 1H), 3.87 (m, 2H), 3.68 (m, 2H), 3.25–3.03 (m, 14H), 2.17 (s, 3H), 1.96–1.34 (m, 11H); MS (ESI): m/z 453 (M + H)⁺.

N-{4-[4-(3-Amino-phenyl)-piperazin-1-yl]-butyl}-C-cyclohexyl-N-methyl-methanesulfonamide (19c). This compound was prepared by the reduction of **18c** in the same manner as compound **19a**, described above, and was purified by silica gel chromatography (eluent 2% MeOH in CH₂Cl₂) (yield 76%); ¹H NMR (CDCl₃): δ 7.28 (s, 1H), 7.23 (t, J = 7.1 Hz, 1H), 6.94 (d, J = 7.0 Hz, 1H), 6.30 (d, J = 7.2 Hz, 1H), 3.85 (sb, 2H), 3.63 (m, 2H), 3.28–3.05 (m, 16H), 2.17 (s, 3H), 1.99–1.39 (m, 11H); MS (ESI): m/z 423 (M + H)⁺.

N-(3-[4-[4-(Cyclohexylmethanesulfonyl-methyl-amino)-butyl]-piperazin-1-yl]-phenyl)-acetamide (20p). This compound (as a white solid) was prepared by **19c** and acetyl chloride in the same manner as compound **20a**, described above, and was purified by silica gel chromatography (eluent 1% MeOH in CH₂Cl₂) (83% yield); ¹H NMR (CDCl₃): δ 7.37 (s, 1H), 7.15 (t, J = 7.4 Hz, 1H), 6.98 (d, J = 7.2 Hz, 1H), 6.71 (d, J = 7.3 Hz, 1H), 3.27 (t, J = 6.3 Hz, 4H), 3.15 (t, J = 6.2 Hz, 2H), 2.89 (d, J = 6.7 Hz, 2H), 2.46 (t, J = 6.3 Hz, 4H), 2.45 (t, J = 6.3 Hz, 2H), 2.23 (s, 3H), 2.19 (s, 3H), 1.99 (t, J = 6.4 Hz, 2H), 1.68 (m, 7H), 1.33–1.02 (m, 6H); MS (ESI): m/z 465 (M + H)⁺. Anal. (C₂₄H₄₀N₄O₃S) C, H, N.

Toluene-4-sulfonic Acid 4-tert-Butoxycarbonylamino-butyl Ester (15a). This compound was prepared with (4-hydroxy-butyl)-carbamic acid *tert*-butyl ester and tosyl chloride in the same manner as compound **13a**, described above, and was used for next step without further purification. MS (ESI): m/z 344 (M + H)⁺.

{4-[4-(3-Nitro-phenyl)-piperazin-1-yl]-butyl}-carbamic Acid *tert*-Butyl Ester (16a). This compound was prepared by alkylation of **11** with **15a** in the same manner as compound **18a**, described above, and was purified by silica gel chromatography (eluent 1% MeOH in CH₂Cl₂) (63% yield); ¹H NMR (CDCl₃): δ 7.78 (s, 1H), 7.67 (d, J = 8.0 Hz, 1H), 7.43–7.40 (m, 1H), 7.21 (d, J = 7.6 Hz, 1H), 5.21 (sb, 1H), 3.39–3.21 (m, 4H), 2.69–2.67 (m, 4H), 2.24–2.20 (m, 2H), 2.19–2.17 (m, 2H), 1.78–1.42 (m, 4H), 1.44 (s, 9H); MS (ESI): m/z 379 (M + H)⁺.

4-[4-(3-Nitro-phenyl)-piperazin-1-yl]-butylamine Trifluoroacetic Acid Salt (17a). To a solution of **16a** (14.0 g, 0.037 mol) in dichloromethane (100 mL) at 0°C trifluoroacetic acid (10 mL, 0.13 mol) was added. The mixture was stirred for additional 2 h. Solvent was evaporated under reduced pressure. The residue was washed with diethyl ether (100 mL). Precipitate was dried to obtain the desired product **17a** (16.85 g, 90% yield); ¹H NMR (CD₃OD): δ 10.05 (sb, 1H), 7.79–7.42 (m, 4H), 4.07–3.48 (m, 4H), 3.25 (sb, 3H), 2.85–2.81 (m, 4H), 2.19–2.15 (m, 2H), 1.99–1.42 (m, 6H); MS (ESI): m/z 279 (M + H)⁺.

Cyclohexanesulfonic Acid {4-[4-(3-Nitro-phenyl)-piperazin-1-yl]-butyl}-amide (18d). This compound was prepared with 4-[4-(3-nitro-phenyl)-piperazin-1-yl]-butylamine trifluoroacetic acid salt (**17a**) and cyclohexanesulfonyl chloride in the same manner as compound **20a**, described above, and was purified by silica gel

chromatography (eluent 1% MeOH in CH₂Cl₂) (61% yield); ¹H NMR (CDCl₃): δ 7.76 (t, J = 2.4 Hz, 1H), 7.71 (t, J = 1.6 Hz, 1H), 7.40 (t, J = 7.7 Hz, 1H), 7.22 (d, J = 2.2 Hz, 1H), 3.49 (t, J = 5.6 Hz, 4H), 3.21 (t, J = 5.2 Hz, 2H), 2.88 (m, 4H), 2.57 (t, J = 5.2 Hz, 4H), 2.45 (t, J = 5.6 Hz, 2H), 1.96–1.20 (m, 14H); MS (ESI): m/z 424 (M + H)⁺.

Cyclohexanesulfonic Acid {4-[4-(3-Amino-phenyl)-piperazin-1-yl]-butyl}-amide (19d). This compound was prepared by reduction of **18d** in the same manner as compound **19a**, described above, and was purified by silica gel chromatography (eluent 2% MeOH in CH₂Cl₂) (75% yield); ¹H NMR (CDCl₃): δ 7.34 (m, 1H), 7.11 (m, 1H), 6.35 (m, 2H), 3.27 (t, J = 5.6 Hz, 4H), 3.02 (t, J = 5.2 Hz, 2H), 2.79 (m, 4H), 2.60 (t, J = 5.2 Hz, 4H), 2.49 (t, J = 5.6 Hz, 2H), 1.99–1.12 (m, 14H); MS (ESI): m/z 394 (M + H)⁺.

N-(3-(4-(4-(Cyclohexylsulfonylamino)butyl)piperazin-1-yl)-phenyl)acetamide (20k). This compound was prepared by using **19d** and acetyl chloride in the same manner as compound **20a**, described above, and was purified by silica gel chromatography (eluent 1% MeOH in CH₂Cl₂) (95% yield); ¹H NMR (CDCl₃): δ 7.36 (t, J = 1.6 Hz, 1H), 7.28 (t, J = 1.6 Hz, 1H), 6.91 (d, J = 7.7 Hz, 1H), 6.73 (d, J = 2.2 Hz, 1H), 3.28 (t, J = 5.6 Hz, 4H), 3.18 (t, J = 5.2 Hz, 2H), 2.86 (m, 1H), 2.66 (t, J = 5.2 Hz, 4H), 2.49 (t, J = 5.6 Hz, 2H), 2.21 (s, 3H), 1.99–1.12 (m, 14H); MS (ESI): m/z 437 (M + H)⁺. Anal. (C₂₂H₃₆N₄O₃S) C, H, N.

Propane-2-sulfonic Acid {4-[4-(3-Nitro-phenyl)-piperazin-1-yl]-butyl}-amide (18e). This compound was prepared with 4-[4-(3-nitro-phenyl)-piperazin-1-yl]-butylamine trifluoroacetic acid salt (**17a**) and propane-2-sulfonyl chloride in the same manner as compound **20a**, described above, and was purified by silica gel chromatography (eluent 1% MeOH in CH₂Cl₂) (63% yield); ¹H NMR (CDCl₃): δ 7.81–7.69 (m, 2H), 7.44–7.22 (m, 2H), 6.60 (sb, 1H), 3.44–3.33 (m, 4H), 3.24–3.13 (m, 3H), 2.75–2.64 (m, 4H), 2.58–2.50 (m, 2H), 1.77–1.70 (m, 4H), 1.40 (d, J = 6.8 Hz, 6H); MS (ESI): m/z 385 (M + H)⁺.

Propane-2-sulfonic Acid {4-[4-(3-Amino-phenyl)-piperazin-1-yl]-butyl}-amide (19e). This compound was prepared by reduction of **18e** in the same manner as compound **19a**, described above, and was purified by silica gel chromatography (eluent 2% MeOH in CH₂Cl₂) (70% yield); ¹H NMR (CDCl₃): δ 7.06–7.02 (m, 1H), 6.36 (d, J = 7.6 Hz, 1H), 6.26–6.21 (m, 2H), 3.60 (sb, 2H), 3.22–3.01 (m, 7H), 2.63–2.61 (m, 4H), 2.50–2.44 (m, 2H), 1.70–1.64 (m, 4H), 1.34 (d, J = 6.8 Hz, 6H); MS (ESI): m/z 355 (M + H)⁺.

N-(3-[4-[4-(Propane-2-sulfonylamino)butyl]-piperazin-1-yl]-phenyl)-acetamide (20l). This compound was prepared with **19e** and acetyl chloride in the same manner as compound **20a**, described above, and was purified by silica gel chromatography (eluent 1% MeOH in CH₂Cl₂) (91% yield); ¹H NMR (CDCl₃): δ 7.32–7.21 (m, 2H), 6.92 (d, J = 7.6 Hz, 1H), 6.71 (d, J = 8.0 Hz, 2H), 3.29–3.11 (m, 7H), 2.67–2.66 (m, 4H), 2.50–2.48 (m, 2H), 2.22 (s, 3H), 1.77–1.66 (m, 4H), 1.39 (d, J = 6.8 Hz, 6H); MS (ESI): m/z 397 (M + H)⁺. Anal. (C₁₉H₃₂N₄O₃S) C, H, N.

C-Cyclohexyl-N-{4-[4-(3-nitro-phenyl)-piperazin-1-yl]-butyl}-methanesulfonamide (18f). This compound was prepared with 4-[4-(3-nitro-phenyl)-piperazin-1-yl]-butylamine trifluoroacetic acid salt (**17a**) and cyclohexyl-methanesulfonyl chloride in the same manner as compound **20a**, described above, and was purified by silica gel chromatography (eluent 2% MeOH in CH₂Cl₂) (88% yield); ¹H NMR (CDCl₃): δ 7.45 (s, 1H), 7.22–7.20 (m, 1H), 6.97 (d, J = 8.0 Hz, 1H), 6.75 (d, J = 7.6 Hz, 1H), 3.87–3.84 (m, 2H), 3.65–3.63 (m, 2H), 3.28–3.05 (m, 14H), 1.99–1.39 (m, 12H); MS (ESI): m/z 439 (M + H)⁺.

N-{4-[4-(3-Amino-phenyl)-piperazin-1-yl]-butyl}-C-cyclohexyl-methanesulfonamide (19f). This compound was prepared by the reduction of **18f** in the same manner as compound **18a**, described above, and was purified by silica gel chromatography (eluent 2% MeOH in CH₂Cl₂) (76% yield); ¹H NMR (CDCl₃): δ 7.50 (s, 1H), 7.13–7.10 (m, 1H), 6.89 (d, J = 8.0 Hz, 1H), 6.69 (d, J = 7.6 Hz, 1H), 3.85 (sb, 2H), 3.65–3.63 (m, 2H), 3.35–3.02 (m, 16H), 2.01–1.44 (m, 12H); MS (ESI): m/z 409 (M + H)⁺.

N-(3-[4-(4-Cyclohexylmethanesulfonylamino)butyl]-piperazin-1-yl)-phenyl)-acetamide (20m). This compound was prepared by

using **19f** and acetyl chloride in the same manner as compound **20a**, described above, and was purified by silica gel chromatography (eluent 1% MeOH in CH₂Cl₂) (89% yield); mp 200.4 °C; ¹H NMR (CDCl₃): δ 7.44 (s, 1H), 7.30 (s, 1H), 7.22–7.20 (m, 1H), 6.93 (d, *J* = 7.6 Hz, 1H), 6.70 (sb, 1H), 6.68 (d, *J* = 8.0 Hz, 1H), 3.28–7.25 (m, 4H), 3.15 (t, *J* = 5.2 Hz, 2H), 2.89 (d, *J* = 6.0 Hz, 2H), 2.64–2.62 (m, 4H), 2.45 (t, *J* = 5.6 Hz, 2H), 2.19 (s, 3H), 2.01–1.97 (m, 2H), 1.68 (m, 7H), 1.33–1.02 (m, 6H); MS (ESI): *m/z* 451 (M + H)⁺. Anal. (C₂₃H₃₈N₄O₃S) C, H, N.

Cyclopropanecarboxylic Acid {3-[4-(4-Cyclohexylmethanesulfonylamino-butyl)-piperazin-1-yl]-phenyl}-amide (20n). This compound was prepared by using **19f** and cyclopropanecarbonyl chloride in the same manner as compound **20a**, described above, and was purified by silica gel chromatography (eluent 1% MeOH in CH₂Cl₂) (89% yield); ¹H NMR (CDCl₃): δ 7.41–7.17 (m, 2H), 6.82 (d, *J* = 7.6 Hz, 1H), 6.65 (d, *J* = 8.0 Hz, 1H), 3.26–3.22 (m, 4H), 3.07–3.03 (m, 4H), 2.89–2.85 (m, 4H), 2.64–2.60 (m, 4H), 2.43–2.40 (m, 2H), 1.95–1.49 (m, 13H), 1.38–0.91 (m, 5H); MS (APCI): *m/z* 477 (M + H)⁺. Anal. (C₂₅H₄₀N₄O₃S) C, H, N.

2-Methyl-propane-1-sulfonic Acid {4-[4-(3-Nitro-phenyl)-piperazin-1-yl]-butyl}-amide (18g). This compound was prepared with 4-[4-(3-nitro-phenyl)-piperazin-1-yl]-butylamine trifluoroacetic acid salt (**17a**) and 2-methyl-propane-1-sulfonyl chloride in the same manner as compound **20a**, described above, and was used for next step without further purification; MS (ESI): *m/z* 399 (M + H)⁺.

2-Methyl-propane-1-sulfonic Acid {4-[4-(3-Amino-phenyl)-piperazin-1-yl]-butyl}-amide (19g). This compound was prepared by reducing **18g** in the same manner as compound **19a**, described above, and was purified by silica gel chromatography (eluent 2% MeOH in CH₂Cl₂) (79% yield); ¹H NMR (CDCl₃): δ 7.05–7.01 (m, 1H), 6.37–6.34 (m, 1H), 6.25–6.20 (m, 2H), 3.21–3.18 (m, 4H), 3.08 (t, *J* = 5.6 Hz, 2H), 2.85 (d, *J* = 6.4 Hz, 2H), 2.61–2.85 (m, 4H), 2.42 (t, *J* = 6.4 Hz, 2H), 2.27–2.16 (m, 1H), 1.68–1.61 (m, 4H), 1.08 (d, *J* = 7.2 Hz, 6H); MS (ESI): *m/z* 369 (M + H)⁺.

N-[3-[4-[4-(2-Methyl-propane-1-sulfonylamino)-butyl]-piperazin-1-yl]-phenyl]-acetamide (20o). This compound was prepared with **19g** and acetyl chloride in the same manner as compound **20a**, described above, and was purified by silica gel chromatography (eluent 1% MeOH in CH₂Cl₂) (93% yield); ¹H NMR (CDCl₃): δ 7.21 (s, 1H), 7.04–7.00 (m, 1H), 6.87 (d, *J* = 7.2 Hz, 1H), 6.66 (d, *J* = 8.4 Hz, 1H), 3.21–3.18 (m, 4H), 3.08 (t, *J* = 6.0 Hz, 2H), 2.85 (d, *J* = 6.4 Hz, 2H), 2.61–2.59 (m, 4H), 2.42 (t, *J* = 6.0 Hz, 2H), 2.27–2.20 (m, 1H), 1.68–1.61 (m, 4H), 1.08 (d, *J* = 6.8 Hz, 6H); MS (ESI): *m/z* 411 (M + H)⁺. Anal. (C₂₀H₃₄N₄O₃S) C, H, N.

Toluene-4-sulfonic Acid 4-(tert-Butoxycarbonyl-methyl-amino)-butyl Ester (15b). This compound was prepared with *tert*-butyl 4-hydroxybutylmethylcarbamate and tosyl chloride in the same manner as compound **13a**, described above, and was used for next step without further purification. MS (ESI): *m/z* 358 (M + H)⁺.

Methyl-[4-[4-(3-nitro-phenyl)-piperazin-1-yl]-butyl]-carbamate Acid tert-Butyl Ester (16b). This compound was prepared with **11** and **15b** in the same manner as compound **18a**, described above, and was purified by silica gel chromatography (eluent 1% MeOH in CH₂Cl₂) (51% yield); ¹H NMR (CDCl₃): δ 7.75 (s, 1H), 7.63 (m, 1H), 7.34 (m, 1H), 7.19 (m, 1H), 3.47 (m, 4H), 2.68 (m, 4H), 2.37 (s, 3H), 2.23 (m, 2H), 2.17 (m, 2H), 1.88–1.45 (m, 4H), 1.44 (s, 9H); MS (ESI): *m/z* 393 (M + H)⁺.

Methyl-[4-[4-(3-nitro-phenyl)-piperazin-1-yl]-butyl]-amine Tri-fluoroacetic Acid Salt (17b). This compound was prepared with **16b** in the same manner as compound **17a**, described above, and was used for next step without further purification; ¹H NMR (CD₃-OD): δ 7.75 (s, 1H), 7.53 (m, 1H), 7.25 (m, 1H), 7.09 (m, 1H), 4.56 (sb, 3H), 3.48 (m, 4H), 2.78 (m, 4H), 2.27 (s, 3H), 2.13 (m, 2H), 1.99–1.45 (m, 6H); MS (ESI): *m/z* 293 (M + H)⁺.

2-Methyl-propane-1-sulfonic Acid Methyl-[4-[4-(3-nitro-phenyl)-piperazin-1-yl]-butyl]-amide (18h). This compound was prepared with methyl-[4-[4-(3-nitro-phenyl)-piperazin-1-yl]-butyl]-amine trifluoroacetic acid salt (**17b**) and 2-methyl-propane-1-sulfonyl chloride in the same manner as compound **20a**, described above, and was purified by silica gel chromatography (eluent 1% MeOH

in CH₂Cl₂) (75% yield); ¹H NMR (CDCl₃): δ 7.26 (s, 1H), 7.12 (t, *J* = 7.3 Hz, 1H), 6.96 (d, *J* = 7.4 Hz, 1H), 6.77 (d, *J* = 7.2 Hz, 1H), 3.89 (m, 2H), 3.65 (m, 2H), 3.29–3.02 (m, 14H), 2.17 (s, 3H), 1.97–1.34 (m, 7H); MS (ESI): *m/z* 413 (M + H)⁺.

2-Methyl-propane-1-sulfonic Acid {4-[4-(3-Amino-phenyl)-piperazin-1-yl]-butyl}-methyl-amide (19h). This compound was prepared by the reduction of **18h** in the same manner as compound **19a**, described above, and was purified by silica gel chromatography (eluent 2% MeOH in CH₂Cl₂) (73% yield); ¹H NMR (CDCl₃): δ 7.27 (s, 1H), 7.13 (t, *J* = 7.5 Hz, 1H), 6.95 (d, *J* = 7.4 Hz, 1H), 6.74 (d, *J* = 7.5 Hz, 1H), 3.95 (sb, 2H), 3.21–3.18 (m, 4H), 3.08 (t, *J* = 6.3 Hz, 2H), 2.85 (d, *J* = 6.0 Hz, 2H), 2.61–2.85 (m, 4H), 2.42 (t, *J* = 6.3 Hz, 2H), 2.29 (s, 3H), 2.27–2.16 (m, 1H), 1.68–1.61 (m, 4H), 1.08 (d, *J* = 6.4 Hz, 6H); MS (ESI): *m/z* 383 (M + H)⁺.

N-[3-(4-[4-[Methyl-(2-methyl-propane-1-sulfonyl)-amino]-butyl]-piperazin-1-yl]-phenyl)-acetamide (20q). This compound was prepared with **19h** and acetyl chloride in the same manner as compound **20a**, described above, and was purified by silica gel chromatography (eluent 1% MeOH in CH₂Cl₂) (91% yield); ¹H NMR (CDCl₃): δ 7.47 (s, 1H), 7.23 (m, 1H), 6.98 (d, *J* = 7.4 Hz, 1H), 6.73 (d, *J* = 8 Hz, 1H), 3.21–3.18 (m, 4H), 3.12 (t, *J* = 6.7 Hz, 2H), 2.82 (d, *J* = 6.3 Hz, 2H), 2.63–2.60 (m, 4H), 2.45 (t, *J* = 6.2 Hz, 2H), 2.31 (s, 3H), 2.27–2.20 (m, 1H), 1.68–1.61 (m, 4H), 1.08 (d, *J* = 6.4 Hz, 6H); MS (ESI): *m/z* 425 (M + H)⁺. Anal. (C₂₁H₃₆N₄O₃S) C, H, N.

4-(Toluene-4-sulfonyloxymethyl)-piperidine-1-carboxylic Acid tert-Butyl Ester (23). This compound was prepared with 4-hydroxymethyl-piperidine-1-carboxylic acid *tert*-butyl ester (**22**) and tosyl chloride in the same manner as compound **13a**, described above, and was used for next step without further purification. MS (ESI): *m/z* 370 (M + H)⁺.

4-[4-(3-Nitro-phenyl)-piperazin-1-ylmethyl]-piperidine-1-carboxylic Acid tert-butyl Ester (24). This compound was prepared with **23** and **11** in the same manner as compound **18a**, described above, and was purified by silica gel chromatography (eluent 1% MeOH in CH₂Cl₂) (92% yield); ¹H NMR (CDCl₃): δ 7.30–6.69 (m, 4 H), 3.80–3.61 (m, 4 H), 3.21–3.19 (m, 4 H), 2.51–2.49 (m, 4 H), 2.23 (d, *J* = 7.6 Hz, 2 H), 1.80–1.59 (m, 5 H), 1.39 (s, 9 H); MS (ESI): *m/z* 405 (M + H)⁺.

1-(3-Nitro-phenyl)-4-piperidin-4-ylmethyl-piperazine Tri-fluoroacetic Acid Salt (25). This compound was prepared with **24** in the same manner as compound **17a**, described above, and was used for next step without further purification; MS (ESI): *m/z* 305 (M + H)⁺.

1-(1-Cyclohexylmethanesulfonyl)-piperidin-4-ylmethyl)-4-(3-nitrophenyl)-piperazine (26a). This compound was prepared with **25** and cyclohexyl-methanesulfonyl chloride in the same manner as compound **20a**, described above, and was purified by silica gel chromatography (eluent 1% MeOH in CH₂Cl₂) (90% yield); ¹H NMR (CDCl₃): δ 7.30–6.66 (m, 4 H), 3.90–3.52 (m, 2 H), 3.22–3.19 (m, 4 H), 3.02 (d, *J* = 6.4 Hz, 2 H), 2.51–2.49 (m, 4 H), 2.21 (d, *J* = 7.6 Hz, 2 H), 1.98–1.22 (m, 16 H); MS (ESI): *m/z* 465 (M + H)⁺.

3-[4-[(1-Cyclohexylmethanesulfonyl)-piperidin-4-ylmethyl)-piperazin-1-yl]-phenylamine (27a). This compound was prepared by the reduction of **26a** in the same manner as compound **19a**, described above, and was purified by silica gel chromatography (eluent 2% MeOH in CH₂Cl₂) (95% yield); ¹H NMR (CDCl₃): δ 7.79–7.77 (m, 1 H), 7.30–7.39 (m, 3 H), 3.88–3.85 (m, 2 H), 3.61 (br s, 2 H), 3.22–3.19 (m, 4 H), 3.02 (d, *J* = 6.4 Hz, 2 H), 2.51–2.48 (m, 4 H), 2.20 (d, *J* = 7.6 Hz, 2 H), 1.90–1.20 (m, 16 H); MS (ESI): *m/z* 435 (M + H)⁺.

N-[3-[4-(1-Cyclohexylmethanesulfonyl)-piperidin-4-ylmethyl)-piperazine-1-yl]-phenyl]-acetamide (21a). This compound was prepared with **27a** and acetyl chloride in the same manner as compound **20a**, described above, and was purified by silica gel chromatography (eluent 1% MeOH in CH₂Cl₂) (91% yield); ¹H NMR (CDCl₃): δ 7.30–6.60 (m, 4 H), 3.87–3.50 (m, 4 H), 3.21–3.19 (m, 4 H), 3.02 (d, *J* = 6.4 Hz, 2 H), 2.52–2.50 (m, 4 H), 2.22

(d, $J = 7.6$ Hz, 2 H), 2.15 (s, 3 H), 2.00–1.20 (m, 16 H); MS (ESI): m/z 477 (M + H)⁺. Anal. (C₂₅H₄₀N₄O₃S) C, H, N.

1-(3-Nitro-phenyl)-4-[1-(propane-2-sulfonyl)-piperidin-4-ylmethyl]-4-piperazine (26b). This compound was prepared with **25** and propane-2-sulfonyl chloride in the same manner as compound **20a**, described above, and was purified by silica gel chromatography (eluent 1% MeOH in CH₂Cl₂) (96% yield); ¹H NMR (CDCl₃): δ 7.30–6.61 (m, 4 H), 3.86–3.20 (m, 4 H), 3.23–3.19 (m, 4 H), 3.25–3.23 (m, 1 H), 2.53–2.51 (m, 4 H), 2.21 (d, $J = 7.6$ Hz, 2 H), 1.88–1.41 (m, 5 H), 1.39 (d, $J = 6.4$ Hz, 6H); MS (ESI): m/z 411.3 (M + H)⁺.

3-{4-[1-(Propane-2-sulfonyl)-piperidin-4-ylmethyl]-piperazin-1-yl}-phenylamine (27b). This compound was prepared by the reduction of **26b** in the same manner as compound **19a**, described above, and was purified by silica gel chromatography (eluent 2% MeOH in CH₂Cl₂) (95% yield); ¹H NMR (CDCl₃): δ 7.78–7.77 (m, 1 H), 7.31–6.61 (m, 3 H), 3.86–3.20 (m, 4 H), 3.23–3.19 (m, 4 H), 3.24–3.22 (m, 1 H), 2.53–2.50 (m, 4 H), 2.21 (d, $J = 7.6$ Hz, 2 H), 1.87–1.40 (m, 5 H), 1.39 (d, $J = 6.4$ Hz, 6H); MS (ESI): m/z 381 (M + H)⁺.

N-(3-{4-[1-(Propane-2-sulfonyl)-piperidin-4-ylmethyl]-piperazine-1-yl}-phenyl)-acetamide (21b). This compound was prepared with **27b** and acetyl chloride in the same manner as compound **20a**, described above, and was purified by silica gel chromatography (eluent 1% MeOH in CH₂Cl₂) (92% yield); ¹H NMR (CDCl₃): δ 7.32–6.60 (m, 4 H), 3.88–3.22 (m, 4 H), 3.22–3.19 (m, 4 H), 3.25–3.22 (m, 1 H), 2.54–2.52 (m, 4 H), 2.21 (d, $J = 7.6$ Hz, 2 H), 2.16 (s, 3 H), 1.87–1.41 (m, 5 H), 1.38 (d, $J = 6.4$ Hz, 6H); MS (ESI): m/z 423 (M + H)⁺. Anal. (C₂₁H₃₄N₄O₃S) C, H, N.

1-[1-(4-Fluoro-benzenesulfonyl)-piperidin-4-ylmethyl]-4-(3-nitro-phenyl)-piperazine (26c). This compound was prepared with **25** and 4-fluoro-benzenesulfonyl chloride in the same manner as compound **20a**, described above, and was purified by silica gel chromatography (eluent 1% MeOH in CH₂Cl₂) (95% yield); ¹H NMR (CDCl₃): δ 7.79–7.75 (m, 2H), 7.27–7.18 (m, 3 H), 6.40–6.38 (m, 3 H), 3.22–3.20 (m, 4 H), 2.52–2.49 (m, 4 H), 2.20 (d, $J = 7.6$ Hz, 2 H), 1.88–1.39 (m, 5 H); MS (ESI): m/z 463 (M + H)⁺.

3-{4-[4-Fluoro-benzenesulfonyl)-piperidin-4-ylmethyl]-piperazin-1-yl}-phenylamine (27c). This compound was prepared by the reduction of **26c** in the same manner as compound **19a**, described above, and was purified by silica gel chromatography (eluent 2% MeOH in CH₂Cl₂) (97% yield); ¹H NMR (CDCl₃): δ 7.81–7.99 (m, 2H), 7.24–7.00 (m, 3 H), 6.39–6.20 (m, 3 H), 3.81–3.79 (m, 2 H), 3.60 (br s, 2 H), 3.22–3.20 (m, 4 H), 2.52–2.49 (m, 4 H), 2.25–2.22 (m, 2 H), 2.20 (d, $J = 7.6$ Hz, 2 H), 1.88–1.39 (m, 5 H); MS (ESI): m/z 433 (M + H)⁺.

N-(3-{4-[4-(Fluoro-benzenesulfonyl)-cyclohexyl]-piperazin-1-yl)-acetamide (21c). This compound was prepared with **27c** and acetyl chloride in the same manner as compound **20a**, described above, and was purified by silica gel chromatography (eluent 1% MeOH in CH₂Cl₂) (94% yield); ¹H NMR (CDCl₃): δ 7.85–7.83 (m, 2H), 7.47–7.46 (m, 1 H), 7.38–7.22 (m, 3 H), 6.95 (d, $J = 8$ Hz, 1 H), 6.78 (d, $J = 7.6$ Hz, 1 H), 3.78–3.60 (m, 4 H), 3.20 (m, 4 H), 2.52–2.49 (m, 4 H), 2.22 (d, $J = 7.6$ Hz, 2 H), 2.21 (s, 3 H), 1.70–1.52 (m, 5 H); MS (ESI): m/z 475.2 (M + H)⁺. Anal. (C₂₄H₃₁N₄O₃S) C, H, N.

In Vitro Pharmacology. Screening Radioligand Binding. The selected compounds were purchased from the respective vendors and experimentally tested in vitro for binding to the 5-HT_{1A} receptor using a radioligand displacement assay performed by CEREP (Paris, France). Compounds were initially tested at a 10 μ M concentration in duplicates. Hits showing more than 50% inhibition at 10 μ M were validated by a full concentration dose response curve, measured between 10⁻¹⁰ and 10⁻⁴ M. Compounds with experimentally validated binding affinities lower than 5 μ M are defined as actual hits.

Radioligand Binding Studies. All radioligand binding studies were performed by CEREP (Paris, France) or MDS Pharma Services (Taiwan, Republic of China). All studies were initially carried out at 1 μ M in duplicates, unless otherwise indicated in the results. In

cases where >50% displacement was observed, specific K_i values were determined ($n = 2$). 67 binding sites were examined, including other 5-HT receptors, biogenic amine receptors, other GPCRs, ion channels, and transporters. The majority of assays were performed using a human recombinant receptor. Where a human assay system was unavailable, receptor binding was performed in tissue from mouse, rat, guinea pig, chicken, or bovine source.

[³⁵S]GTP γ S Binding Studies. Studies were performed by MDS Pharma Services (Taiwan, Republic of China). Assays were performed in triplicates ($n = 3$) and nonspecific binding was determined in the presence of 100 μ M GTP γ S.

hERG Binding Assay. The ability to block the hERG (K⁺) channel was evaluated in HEK-293 cells stably expressing hERG (human ether-a-go-go related gene) by the whole-cell patch clamp method. The degree of inhibition (%) was obtained by measuring the tail current amplitude before and after drug perfusion at 1 μ M ($n = 2$).

HLM Microsomes. The metabolic stability of compounds in the presence of human liver microsomes was evaluated at 5 μ M, measured by LC/MS following 0, 15, 30, 45, 60, and 90 min of incubation with human liver microsomes (1.0 mg protein/mL) at 37°C.

LC/MS/MS metabolite identification was performed on the 30 min time point samples.

S9 Assay. The metabolic stability was evaluated in the presence of human liver S9 fraction (with 2 mM NADPH) at a concentration of 5 μ M, measured by LC/MS following 0, 15, 30, 45, 60, and 90 min of incubation with pooled human liver S9 fraction (0.25–10 mg protein/mL) at 37°C.

Cytochrome P450 Isoenzyme Inhibition. The inhibition of human recombinant cytochrome P450 enzyme activity (isoenzymes 1A2, 2C9, 2C19, 2D6, and 3A4) was determined in this assay. Enzyme activity was measured using fluorogenic substrates {3-cyano-7-ethoxycoumarin, 7-methoxy-4-trifluoromethylcoumarin, 3-[2-(*N,N*-diethyl-*N*-methylamino)ethyl]-7-methoxy-4-methylcoumarin, 7-benzyloxyquinoline, and 7-benzyloxy-4-(trifluoromethyl)-coumarin} in the absence and presence of the compound. The isoenzyme incubations were performed in the presence of an NADPH regenerating system (glucose-6-phosphate/glucose-6-phosphate dehydrogenase) at approximately 20°C for 30 min over a range of 10 concentrations (at 1:4 serial dilutions from 30 mM). The IC₅₀ values were calculated using a standard 4 parameter curve fit.

Human Hepatocytes Stability Assay. The metabolic stability in the presence of human hepatocytes was evaluated at a concentration of 5 μ M, measured by LC/MS following 0, 30, 60, 90, 120, and 180 min of incubation with human cryopreserved hepatocytes at 37°C.

In Vivo Studies. Drugs. 20m (Lot # DC-006-022-L2, C₂₃H₃₈N₄O₃S₂·HCl, doses expressed in mg of salt), buspirone (3, 10, and 20 mg/kg, Sigma, Lot # 101H0402). All compounds were dissolved in sterile injectable water, which served as the vehicle control. All solutions were prepared on the day of the experiments. **20m** was given to animals orally (po) in a volume of 10 mL/kg body weight; buspirone was given to animals intraperitoneally (ip). Test compounds were administered to the animals one hr before testing.

Animals. Male 129S6/SvEvTac mice from Taconic, Germantown, NY, were used in the stress-induced hyperthermia test. Mice were 6 weeks of age upon arrival and were group housed in polycarbonate cages with filter tops for 7 days prior to testing. A 12-h light/dark cycle (lights on 7:00 a.m.) was maintained in the temperature and humidity controlled animal room (20–23°C and 30%–70%, respectively). Chow and water were provided ad libitum. In each test, animals were randomly assigned across treatment groups and balanced by cage number. Ten animals were used in each treatment group. Mice were handled once daily for 2 consecutive days prior to testing.

Stressed Induced Hyperthermia (SIH). The study was carried out during the daytime portion of the light cycle. The test involves two measures of rectal temperature repeated in the same animal

within a 10 min period. On the day prior to testing, animals were brought to the experimental room 1 h prior to scheduled lights out and singly housed overnight with food and water ad libitum. On the morning of the experiment, animals were first injected with treatment compound or vehicle. After 1 h posttreatment, the animal was removed from the holding cage and held in a supine position and had rectal temperature measured by using a rectal probe attached to a PhysiTemp thermometer (Fisher Scientific). For each animal tested, the rectal probe was cleaned with an alcohol pad and lubricated with sterile K–Y jelly and slowly inserted into the animal's rectum at a length of approximately 3–5 mm. The probe remained within the animal's rectum for approximately 5 s or until body temperature reached stability, and the baseline rectal temperature (T1) was recorded. The animal was immediately placed back to the holding cage, and after a 10-min interval a second rectal temperature (T2) was taken using the same procedure as T1. The animal was then returned to the home cage and at the completion of the experiment returned to the colony room.

All data were analyzed by comparing the groups treated with the test substance to the vehicle control or reference treated groups. Statistical analysis was performed by ANOVA followed by Fisher's post-hoc test where appropriate. Statistical significance was established at a *p* value of <0.05. Data are represented as the means and standard error of the mean (SEM).

Rat and Dog PK Studies. The pharmacokinetic properties were investigated in male Sprague–Dawley rats following both intravenous and oral administration. Six animals (three per group) were fasted overnight. On day 1, Group 1 animals were administered the compound intravenously at 1 mg/kg in a dose volume of 0.5 mL/kg. Group 2 animals were administered the compound at 3 mg/kg in a dose volume of 1.5 mL/kg. Serial blood collections were performed at 0.083, 0.25, 0.5, 1, 2, 4, 6, 8, 12, and 24 h following intravenous dosing, and at 0.25, 0.5, 1, 2, 4, 6, 8, 12, and 24 following oral administration from the cannulated jugular vein (or via retroorbital bleed or tail vein depending upon cannula patency). On day 2, all animals were dose as described above followed by blood and brain collection at 1 hour post dose. On days 1 and 2 all animals were observed for clinical signs. Presence of the compound, in both blood and brain, was measured by LC/MS.

The pharmacokinetic properties were investigated in male beagle dogs following both intravenous and oral administration. Three animals were fasted overnight and on day 1 were administered the compound intravenously at a dose level of 1 mg/kg in a dose volume of 1 mL/kg. On day 2 the compound was administered orally at a dose level of 3 mg/kg in a dose volume of 5 mL/kg. Serial blood collections were performed at 5, 15, 30 min and 1, 2, 4, 6, 8, 12, and 24 h following intravenous administration; and 15 and 30 min and 1, 2, 4, 6, 8, 12, and 24 following oral administration from a cephalic or jugular vein. On days 1 and 2, animals were observed for clinical signs. Plasma levels was measured by LC/MS.

Noncompartmental pharmacokinetic analysis of the plasma concentration vs time data was performed using Watson software (version 5.4.1.04).

Acknowledgment. We thank our clinical drug development operations team members, Christine Wang, Alexandra Petrusich, and Steve Potter. We also thank Kimberley Gannon, Stephen Donahue, Joseph Rutkowski, and Adam Muzikant for significant assistance in preparing this manuscript.

References

- Page, I. H. Serotonin (5-hydroxytryptamine). *Physiol. Rev.* **1954**, *34*, 563–88.
- Glennon, R. A. Serotonin Receptor: Clinical Implications. *Neurosci. Biobehav. Rev.* **1990**, *14*, 35–47.
- Wilkinson, L. O.; Dourish, C. T. *Serotonin Receptor Subtypes: Basic and Clinical Aspects*; Peroutka, S., Ed.; John Wiley and Sons: New York, 1991; p 147.
- Winsauer, P. J.; Rodrigues, F. H.; Cha, A. E.; Moerschbacher, Full and partial 5-HT_{1A} receptor agonists disrupt learning and performance in rats. *J. M. Pharmacol. Exp. Ther.* **1999**, *288*, 3335–347.
- Baumgarten, H. G.; Göthert, M., Eds. *Serotonergic Neurons and 5-HT Receptors in the CNS: Handbook of Experimental Pharmacology*, Vol. 129; Springer-Verlag: Berlin, 1997.
- Martin, G. R.; Eglén, R. M.; Hoyer, D.; Hamblin, M. W.; Yocca, F., Eds. *Advances in Serotonin Receptor Research: Molecular Biology, Signal Transduction, and Therapeutics*; Annals of the New York Academy of Sciences: New York, 1998.
- Hoyer, D.; Hannon, J. P.; Martin, G. R. Molecular, Pharmacological and Functional Diversity of 5-HT Receptors. *Pharmacol. Biochem. Behav.* **2002**, *71*, 533–554.
- Martin, G. R.; Eglén, R. M.; Hoyer, D.; Hamblin, M. W.; Yocca, F. The structure and signalling properties of 5-HT receptors: an endless diversity? *Trends Pharmacol. Sci.* **1998**, *19*, 2–4.
- De Vry, J.; Schreiber, R.; Glaser, T.; Traber, J. Serotonin 1A receptors in Depression and Anxiety. Stahl, S. M.; Gastpar, M.; Keppel, J. M.; Traber, J., Eds., Raven Press: New York, 1992, p 55.
- De Vry, J. 5-HT_{1A} receptor agonists: recent developments and controversial issues. *Psychopharmacology (Berl)* **1995**, *121*, 1–26.
- Gonzalez, L. E.; File, S. E.; Overstreet, D. H.; Selectively bred lines of rats differ in social interaction and hippocampal 5-HT_{1A} receptor function: a link between anxiety and depression? *Pharmacol. Biochem. Behav.* **1998**, *59*, 787–92.
- Menard, J.; Treit, D. Effects of centrally administered anxiolytic compounds in animal models of anxiety. *Neurosci. Biobehav. Rev.* **1999**, *23*, 591–613.
- Blier, P.; Abbott, F. V. Putative mechanisms of action of antidepressant drugs in affective and anxiety disorders and pain. *J. Psych. Neurosci.* **2001**, *26*, 37–43.
- Nemeroff, C. Anxiolytics: past, present and future agents. *J. Clin. Psych.* **2003**, *64*, 3–6.
- Goldberg, H. L.; Finnerty, R. J. The comparative efficacy of buspirone and diazepam in the treatment of anxiety. *Am. J. Psychiatry* **1979**, *136*, 1184–7.
- Bristol-Myers Squibb Company. Buspar Package Insert, Revised February 2002.
- Sramek, J. J.; Tansman, M.; Suri, A.; Hornig-Rohan, M.; Amsterdam, J. D.; Stahl, S. M.; Weisler, R. H.; Cutler, N. R. Efficacy of buspirone in generalized anxiety disorder with coexisting mild depressive symptoms. *J. Clin. Psychiatry* **1996**, *57*, 287–91.
- Delle Chiaie, R.; Pancheri, P.; Casacchia, M.; Stratta, P.; Kotzalidis, G. D.; Zibellini, M. Assessment of the efficacy of buspirone in patients affected by generalized anxiety disorder, shifting to buspirone from prior treatment with lorazepam: a placebo-controlled, double-blind study. *J. Clin. Psychopharmacol.* **1995**, *15*, 12–9.
- Gammans, R. E.; Stringfellow, J. C.; Hvizdos, A. J.; Seidehamel, R. J.; Cohn, J. B.; Wilcox, C. S.; Fabre, L. F.; Pecknold, J. C.; Smith, W. T.; Rickels, K. Use of buspirone in patients with generalized anxiety disorder and coexisting depressive symptoms. A meta-analysis of eight randomized, controlled studies. *Neuropsychobiology* **1995**, *25*, 193–201.
- Landen, M.; Eriksson, E.; Agren, H.; Fahlen, T. Effect of buspirone on sexual dysfunction in depressed patients treated with selective serotonin reuptake inhibitors. *J. Clin. Psychopharmacol.* **1999**, *19*, 268–71.
- Landen, M.; Eriksson, O.; Sundblad, C.; Andersch, B.; Naessen, T.; Eriksson, E. Compounds with affinity for serotonergic receptors in the treatment of premenstrual dysphoria: a comparison of buspirone, nefazodone and placebo. *Psychopharmacology (Berl)*. **2001**, *155*, 292–8.
- Gammans, R. E.; Mayol, R. F.; LaBudde, J. A. Metabolism and disposition of buspirone. *Am. J. Med.* **1986**, *80*, 41–51.
- Blier, P. The pharmacology of putative early-onset antidepressant strategies. *Eur. Neuropsychopharmacol.* **2003**, *13*, 57–66.
- Feiger, A. D.; Heiser, J. F.; Shrivastava, R. K.; Weiss, K. J.; Smith, W. T.; Sitsen, J. M.; Gibertini, M. Gepirone extended-release: new evidence for efficacy in the treatment of major depressive disorder. *J. Clin. Psychiatry*. **2003**, *64*, 243–9.
- Stahl, S. M.; Kaiser, L.; Roeschen, J.; Keppel Hesselink, J. M.; Orazem, J. Effectiveness of ipsapirone, a 5-HT-1A partial agonist, in major depressive disorder: support for the role of 5-HT-1A receptors in the mechanism of action of serotonergic antidepressants. *Int. J. Neuropsychopharmacol.* **1998**, *1*, 11–18.
- Masuda, Y.; Akagawa, Y.; Hishikawa, Y. Effect of serotonin 1A agonist tandospirone on depression symptoms in senile patients with dementia. *Hum. Psychopharmacol.* **2002**, *17*, 191–3.
- Barbhuiya, R. H.; Shukla, U. A.; Pfeffer, M.; Pittman, K. A.; Shrotriya, R.; Laroudie, C.; Gammans, R. E. Disposition kinetics of buspirone in patients with renal or hepatic impairment after administration of single and multiple doses. *Eur. J. Clin. Pharmacol.* **1994**, *46*, 41–7.
- Timmer C. J.; Sitsen J. M. Pharmacokinetic evaluation of gepirone immediate-release capsules and gepirone extended-release tablets in healthy volunteers. *J. Pharm. Sci.* **2003**, *92*, 1773–8.

- (29) Olivier, B.; Soudijn, W.; van Wijngaarden, I. The 5-HT_{1A} receptor and its ligands: structure and function. *Prog. Drug Res.* **1999**, *52*, 103–65.
- (30) Nelson, D. L. Structure–activity relationships at 5-HT_{1A} receptors: Binding profiles and intrinsic activity. *Pharmacol. Biochem. Behav.* **1991**, *40*, 1041–1051.
- (31) Lopez-Rodriguez, M. L.; Ayala, D.; Benhamu, B.; Morcillo, M. J.; Viso, A. Arylpiperazine derivatives acting at 5-HT_{1A} receptors. *Curr. Med. Chem.* **2002**, *9*, 443–469.
- (32) Glennon, R. A. Concepts for the design of 5-HT_{1A} serotonin agonists and antagonists. *Drug. Dev. Res.* **1992**, *26*, 251–274.
- (33) Peglion, J.-L.; Goument, B.; Despau, N.; Charlot, V.; Giraud, H.; Nisole, C.; Newman-Tancredi, A.; Dekeyne, A.; Bertrand, M.; Genissel, P.; Millan, M. J. Improvement in the selectivity and metabolic stability of the serotonin 5-HT_{1A} ligand, S 15535: A series of *cis*- and *trans*-2-(arylcycloalkylamine)-1-indanols. *J. Med. Chem.* **2002**, *44*, 165–176.
- (34) Bojarski, A. J.; Kowalski, P.; Kowalska, T.; Duszynska, B.; Charakchieva-Minol, S.; Tatarczynska, E.; Klodzinska, A.; Chojnacka-Wojcik, C. Synthesis and Pharmacological Evaluation of New Arylpiperazines. 3-[4-[4-(3-chlorophenyl)-1-piperazinyl]butyl]-quinazolin-4-one: A Dual Serotonin 5-HT_{1A}/5-HT_{2A} Receptor Ligand with an Anxiolytic-Like Activity. *Bioorg. Med. Chem.* **2002**, *10*, 3817–3827.
- (35) Heinrich, T.; Botcher, H.; Bartoszyk, G. D.; Griner, H. E.; Seyfried, C. A.; van Amsterdam, C. Indolebutylamines as Selective 5-HT_{1A} Agonists. *J. Med. Chem.* **2004**, *47*, 4677–4683.
- (36) Heinrich, T.; Botcher, H.; Gericke, R.; Bartoszyk, G. D.; Anzali, S.; Seyfried, C. A.; Griner, H. E.; van Amsterdam, C. Synthesis and Structure–Activity Relationship in a Class of Indolebutylpiperazines as Dual 5-HT_{1A} Receptor Agonists and Serotonin Reuptake Inhibitors. *J. Med. Chem.* **2004**, *47*, 4684–4692.
- (37) Lopez-Rodriguez, M. L.; Rosado, M. L.; Benhamu, B.; Morcillo, M. J.; Sanz, A. M.; Orensanz, L.; Beneitez, M. E.; Fuentes, J. A.; Manzanares, J. Synthesis and Structure–Activity Relationships of a New Model of Arylpiperazines. 1.2-[4-(*o*-Methoxy-phenyl) piperazin-1-ylmethyl]-1,3-dioxoperhydroimidazo[1,5-*a*]pyridine: A Selective 5-HT_{1A} Receptor Agonist. *J. Med. Chem.* **1996**, *39*, 4439–4450.
- (38) Lopez-Rodriguez, M. L.; Rosado, M. L.; Benhamu, B.; Morcillo, M. J.; Fernandez, E.; Schaper, K.-J. Synthesis and Structure–Activity Relationships of a New Model of Arylpiperazines. 2. Three-Dimensional Quantitative Structure–Activity Relationships of New Hydantoin-Phenylpiperazine Derivatives with Affinity for 5-HT_{1A} and α 1 Receptors. A Comparison of CoMFA Models. *J. Med. Chem.* **1997**, *40*, 1648–1656.
- (39) Lopez-Rodriguez, M. L.; Morcillo, M. J.; Fernandez, E.; Porras, E.; Murcia, M.; Sanz, A. M.; Orensanz, L. Synthesis and Structure–Activity Relationships of a New Model of Arylpiperazines. 3. 2-[\ddot{o} -(4-Arylpiperazin-1-yl)alkyl]perhydropyrrolo-[1,2-*c*]imidazoles and –Perhydroimidazo[1,5-*a*]pyridines: Study of the Influence of the Terminal Amide Fragment on 5-HT_{1A} Affinity/Selectivity. *J. Med. Chem.* **1997**, *40*, 2653–2656.
- (40) Lopez-Rodriguez, M. L.; Morcillo, M. J.; Rovat, T. K.; Fernandez, E.; Vicente, B.; Sanz, A. M.; Hernandez, M.; Orensanz, L. Synthesis and Structure–Activity Relationships of a New Model of Arylpiperazines. 4. 1-[*o*-(4-Arylpiperazin-1-yl)alkyl]-3-di-phenylmethylene-2,5-pyrrolidinediones and -3-(9*H*-Fluoren-9-ylidene)-2,5-pyrrolidinediones: Study of the Steric Requirements of the Terminal Amide Fragment on 5-HT_{1A} Affinity/Selectivity. *J. Med. Chem.* **1961**, *42*, 36–49.
- (41) Lopez-Rodriguez, M. L.; Morcillo, M. J.; Fernandez, E.; Porras, E.; Orensanz, L.; Beneytez, M. E.; Manzanares, J.; Fuentes, J. A. Synthesis and Structure–Activity Relationships of a New Model of Arylpiperazines. 5. Study of the Physicochemical Influence of the Pharmacophore on 5-HT_{1A}/ α 1-Adrenergic Receptor Affinity. Synthesis of a New Selective Derivative with Mixed 5-HT_{1A}/D₂ Antagonist Properties. *J. Med. Chem.* **2001**, *44*, 186–197.
- (42) Lopez-Rodriguez, M. L.; Morcillo, M. J.; Fernandez, E.; Rosado, M. L.; Pardo, L.; Schaper, K.-J. Synthesis and Structure–Activity Relationships of a New Model of Arylpiperazines. 6. Study of the 5-HT_{1A}/ α 1-Adrenergic Receptor Affinity by Classical Hansch Analysis, Artificial Neural Networks, and Computational Simulation of Ligand Recognition. *J. Med. Chem.* **2001**, *44*, 198–207.
- (43) Lopez-Rodriguez, M. L.; Ayala, D.; Viso, A.; Benhamu, B.; Fernandez de la Pradilla, R.; Zarza, F.; Ramos, J. A. Synthesis and Structure–Activity Relationships of a New Model of Arylpiperazines. 7. Study of the Influence of Lipophilic Factors at the Terminal Amide Fragment on 5-HT_{1A} Affinity/Selectivity. *Bioorg. Med. Chem.* **2004**, *12*, 1551–1557.
- (44) Lopez-Rodriguez, M. L.; Morcillo, M. J.; Fernandez, E.; Benhamu, B.; Tejada, I.; Ayala, D.; Viso, A.; Campillo, M.; Pardo, L.; Delgado, M.; Manzanares, J.; Fuentes, J. A. Synthesis and structure–activity relationships of a new model of arylpiperazines. 8. Computational simulation of ligand–receptor interaction of 5-HT_{1A}R agonists with selectivity over α -1-adrenoceptors. *J. Med. Chem.* **2005**, *48*, 2548–58.
- (45) Becker, O. M.; Shacham, S.; Marantz, Y.; Noiman, S. Modeling the 3D structure of GPCRs: Advances and application to drug discovery. *Curr. Opin. Drug Discovery Dev.* **2003**, *6*, 3353–361.
- (46) Shacham, S.; Marantz, Y.; Bar-Haim, S.; Kalid, O.; Warshaviak, D.; Avisar, N.; Inbal, B.; Heifetz, A.; Fichman, M.; Topf, M.; Naor, Z.; Noiman, S.; Becker, O. M. PREDICT Modeling and in-silico screening for G-Protein coupled receptors. *Proteins* **2004**, *57*, 51–86.
- (47) Becker, O. M.; Marantz, Y.; Shacham, S.; Inbal, B.; Heifetz, A.; Kalid, O.; Bar-Haim, S.; Warshaviak, D.; Fichman, M.; Noiman, S. 3D G-Protein Coupled Receptors: In Silico Driven Drug Discovery. *Proc. Natl. Acad. Sci.* **2004**, *101*, 11304–11309.
- (48) Jacoby, E.; Fauchere, J. L.; Raimbaud, E.; Ollivier, S.; Michel, A.; Spedding, M. A Three Binding Site Hypothesis for the Interaction of Ligands with Monoamine G Protein-coupled Receptors: Implications for Combinatorial Ligand Design. *Quant. Struct.-Act. Relat.* **1999**, *18*, 561–572.
- (49) Ho, B. Y.; Karschin, A.; Branchek, T.; Davidson, N.; Lester, H. A. The role of conserved aspartate and serine residues in ligand binding and in function of the 5-HT_{1A} receptor: A site-directed mutation study. *FEBS Lett.* **1992**, *312*, 259–262.
- (50) Shi, L.; Javitch, J. A. The binding site of aminergic G protein-coupled receptors: the transmembrane segments and second extracellular loop. *Annu. Rev. Pharmacol. Toxicol.* **2002**, *42*, 437–467.
- (51) Evers, A.; Klabunde, T. Structure-based drug discovery using GPCR homology modeling: successful virtual screening for antagonists of the α -1A adrenergic receptor. *J. Med. Chem.* **2005**, *48*, 1088–97.
- (52) Viskin, S. Long QT syndromes and torsade de pointes. *Lancet* **1999**, *354*, 1625–1633.
- (53) Mitcheson, J. S.; Chen, J.; Lin, M.; Culberson, C.; Sanguinetti, M. C. A structural basis for drug-induced long QT syndrome. *Proc. Natl. Acad. Sci. U.S.A.* **2000**, *97*, 12329–12333.
- (54) Pearlstein, R.; Vaz, R.; Rampe, D. Understanding the Structure–Activity Relationship of the Human Ether-a-go-go-Related Gene Cardiac K(+) Channel. A Model for Bad Behavior. *J. Med. Chem.* **2003**, *46*, 2017–2022.
- (55) Doyle, D. A.; Morais Cabral, J.; Pfuetzner, R. A.; Kuo, A.; Gulbis, J. M. et al. The structure of the potassium channel: molecular basis of K⁺ conduction and selectivity. *Science* **1998**, *280*, 69–77.
- (56) Borsini, F.; Lecci, A.; Volterra, G.; Meli, A. A model to measure anticipatory anxiety in mice? *Psychopharmacology* **1989**, *98*, 207–211.
- (57) Olivier, B.; Zethof, T.; Pattij, T.; van Boogaert, M.; van Oorschot, R.; Leahy, C.; Oosting, R.; Bouwknecht, A.; Veening, J.; van der Gugten, J.; Groenink, L. Stress-induced hyperthermia and anxiety: pharmacological validation. *Eur. J. Pharmacol.* **2003**, *463*, 117–132.
- (58) Brooks, B. R.; Brucoleri, R. E.; Olafson, B. D.; States, D. J.; Swaminathan, S.; Karplus, M. CHARMM: A program for macromolecular energy, minimization, and dynamics calculations. *J. Comput. Chem.* **1983**, *4*, 187–217.
- (59) MacKerell, A. D., Jr.; Bashford, D.; Bellott, R. L.; Dunbrack, R. L., Jr.; Evanseck, J. D.; Field, M. J.; Fischer, S.; Gao, J.; Guo, H.; Ha, S.; Joseph-McCarthy, D.; Kuchnir, L.; Kuczera, K.; Lau, F. T. K.; Mattos, C.; Michnick, S.; Ngo, T.; Nguyen, D. T.; Prodhom, B.; Reiher, W. E., III; Roux, B.; Schlenkrich, M.; Smith, J. C.; Stote, R.; Straub, J.; Watanabe, M.; Wiorkiewicz-Kuczera, J.; Yin, D.; Karplus, M. All-Atom Empirical Potential for Molecular Modeling and Dynamics Studies of Proteins. *J. Phys. Chem. B* **1998**, *102*, 3586–3616.
- (60) CONCORD, Version Tripos St. Louis, MO 63144.
- (61) SYBYL, Version 6.8. Tripos Inc., St. Louis, MO 63144.
- (62) CONFORT, Tripos St. Louis, MO 63144.
- (63) Ewing, T. J.; Makino, S.; Skillman, A. G.; Kuntz, I. D. DOCK 4.0: search strategies for automated molecular docking of flexible molecule databases. *J. Comput.-Aided Mol. Des.* **2001**, *15*, 411–428.
- (64) DOCK, Version 4.0. Molecular Design Institute University of California: San Francisco, CA.
- (65) CSCORE, Tripos St. Louis, MO 63144.
- (66) Maple, J. R.; Hwang, M.-J.; Stockfish, T. P.; Dinur, U.; Waldman, M.; Ewig, C. S.; Hagler, A. T.; Derivation of class II force fields. I. Methodology and quantum force field for the alkyl functional group and alkane molecules. *J. Comput. Chem.* **1994**, *15*, 162–182.